Nestin in immature embryonic neurons affects axon growth cone morphology and Semaphorin3a sensitivity

C. J. Bott[a], C. G. Johnson[b], C. C. Yap[a], N. D. Dwyer[a], K. A. Litwa[b], and B. Winckler[a,*]
[a]Department of Cell Biology, University of Virginia, Charlottesville, VA 22908; [b]Department of Anatomy and Cell Biology, Brody School of Medicine, East Carolina University, Greenville, NC 27834

ABSTRACT **Correct wiring in the neocortex requires that responses to an individual guidance cue vary among neurons in the same location, and within the same neuron over time. Nestin is an atypical intermediate filament expressed strongly in neural progenitors and is thus used widely as a progenitor marker. Here we show a subpopulation of embryonic cortical neurons that transiently express nestin in their axons. Nestin expression is thus not restricted to neural progenitors, but persists for 2–3 d at lower levels in newborn neurons. We found that nestin-expressing neurons have smaller growth cones, suggesting that nestin affects cytoskeletal dynamics. Nestin, unlike other intermediate filament subtypes, regulates cdk5 kinase by binding the cdk5 activator p35. Cdk5 activity is induced by the repulsive guidance cue Semaphorin3a (Sema3a), leading to axonal growth cone collapse in vitro. Therefore, we tested whether nestin-expressing neurons showed altered responses to Sema3a. We find that nestin-expressing newborn neurons are more sensitive to Sema3a in a roscovitine-sensitive manner, whereas nestin knockdown results in lowered sensitivity to Sema3a. We propose that nestin functions in immature neurons to modulate cdk5 downstream of the Sema3a response. Thus, the transient expression of nestin could allow temporal and/or spatial modulation of a neuron's response to Sema3a, particularly during early axon guidance.**

Monitoring Editor
Kozo Kaibuchi
Nagoya University

Received: Aug 7, 2018
Revised: Feb 21, 2019
Accepted: Feb 26, 2019

INTRODUCTION

Proper wiring of the nervous system requires that axonal growth cones respond to a variety of extracellular guidance cues to find their correct targets (Kolodkin and Tessier-Lavigne, 2011). Semaphorin 3a (Sema3a) is one of many diffusible developmental cues and has been shown to repel axons of responsive neuronal populations (Sibbe *et al.*, 2007). Addition of Sema3a to cortical neuron cultures causes rapid filopodial retraction (within 5 min) and ultimately collapse of many axonal growth cones (Dent *et al.*, 2004). Binding of Sema3a to its receptor neuropilin1 and coreceptor PlexinA4 leads to downstream activation of the neuronal serine/threonine kinase cyclin-dependent kinase 5 (cdk5) (Sasaki *et al.*, 2002; Chen *et al.*, 2008; Perlini *et al.*, 2015). Cdk5 is critical for early neuronal development as a regulator of cytoskeleton, trafficking, and membrane dynamics and thus cell morphology (Kawauchi, 2014). Sema3a-activated cdk5 phosphorylates multiple substrates to affect the assembly and dynamics of both the actin and microtubule cytoskeleton and of adhesion components, which results in filopodial retraction and growth cone collapse in vitro (Sasaki *et al.*, 2002; Ng *et al.*, 2013). Not all cortical neurons are repelled by Sema3a, and the molecular mechanisms for this differential responsiveness are under active investigation (Mintz *et al.*, 2008; Carcea *et al.*, 2010; Ip *et al.*, 2011; Wang *et al.*, 2014).

Intermediate filaments are generally thought to provide structure and stability to a cell. In adult neurons, neuronal intermediate

This article was published online ahead of print in MBoC in Press (http://www.molbiolcell.org/cgi/doi/10.1091/mbc.E18-06-0361) on March 6, 2019.

The authors declare no competing financial interests.

Author contributions: C.B. and B.W. conceived and coordinated the study, interpreted the data, and wrote the paper; C.J. and K.A. devised, performed, and analyzed the human IPSC studies (Figure 2B and Supplemental Figure S2A); C.B. devised, performed, and analyzed all other experiments; C.Y. and N.D. provided critical expertise for experimental design, execution, and analysis.

*Address correspondence to: B. Winckler (bwinckler@virginia.edu).

Abbreviations used: ANOVA, analysis of variance; BSA, bovine serum albumin; cdk5, cyclin-dependent kinase 5; DCX, doublecortin; DIV, day(s) in vitro; GFP, green fluorescent protein; IF, immunofluorescence; IHC, immunohistochemistry; INA, alpha-internexin; IPSC, induced pluripotent stem cell; IZ, intermediate zone; NDS, normal donkey serum; NF-M, neurofilament medium; NMJ, neuromuscular junction; NPC, neural progenitor cell; PBS, phosphate-buffered saline; Sema3a, Semaphorin3a; siRNA, small interfering RNA; STED, stimulated emission depletion; WB, Western blot.

filaments, the neurofilaments, play such a structural role to maintain axon caliber (Lariviere and Julien, 2003). In addition to the classic neurofilaments, other intermediate filament subunits are expressed during neural development. Vimentin and nestin are both strongly expressed in neural progenitor cells (NPCs), so much so that nestin expression is widely used as a marker for NPCs. α-Internexin (INA) and neurofilament protein expression, on the other hand, are up-regulated only after neurons differentiate. Neurofilaments, INA, and vimentin (all expressed in CNS neurons) have also been shown to play additional but poorly understood roles in early neuritogenesis (Shea *et al.*, 1993; Shea and Beermann, 1999; Walker *et al.*, 2001; Lee and Shea, 2014). The function of nestin in neurons has not been investigated, because nestin is not thought to be expressed in neurons.

Little is known about nestin's function, even in NPCs, where it is highly expressed (Sahlgren *et al.*, 2006), but it appears to offer some protection from cellular stress. In addition, nestin is often expressed in cancer cells and has well-documented effects on cancer cell migration and invasion by influencing cytoskeletal dynamics and kinase activity (Hyder *et al.*, 2014; Zhao *et al.*, 2014; Liang *et al.*, 2015; Yan *et al.*, 2016). Nestin's developmental function is best understood in muscle, where it acts as a scaffold and regulator for cdk5 at the neuromuscular junction (NMJ). At the NMJ, nestin deletion phenocopies cdk5 deletion (Lin *et al.*, 2005), and nestin is required for the acetylcholine agonist carbachol-induced cdk5 activity (Mohseni *et al.*, 2011; Pallari *et al.*, 2011; Yang *et al.*, 2011). The binding site for the p35/cdk5 complex has been mapped to the unique long C-terminal tail of nestin (Sahlgren *et al.*, 2003, 2006), which is much larger than conventional intermediate filaments (57 kDa vimentin vs. ~300 kDa nestin).

In this work, we show for the first time that nestin has a function in postmitotic newborn cortical neurons. We first characterized the patterns of endogenous nestin expression. As expected, we find that nestin is strongly expressed in NPCs. Unexpectedly, nestin protein can be detected during early, but critical, periods of axon formation and is subsequently lost. Second, we found that depletion of nestin affects the growth cone morphology of immature cortical neurons. Last, we discovered that nestin depletion from cultured neurons decreases their sensitivity to Sema3a in a roscovitine-dependent manner. On the basis of our data, we propose that nestin acts as a "gain control" modulator of Sema3a growth cone signaling during early neuronal differentiation. Because neurons can encounter the same cue at different developmental stages, but respond differently (Kolodkin and Tessier-Lavigne, 2011), nestin's modulation of Sema3a responsiveness might be one mechanism to temporally and spatially regulate differential axon guidance decisions in the cortex.

RESULTS

Nestin protein expression persists in immature primary cortical neurons in culture

Nestin protein is expressed at high levels in cortical radial glia/neural progenitor cells (NPCs) (Lendahl *et al.*, 1990). In contrast, doublecortin (DCX) and βIII-tubulin expression is low or absent in NPCs but up-regulated in postmitotic neurons (Francis *et al.*, 1999). Nestin and DCX/βIII-tubulin are thus routinely used as markers to distinguish these mutually exclusive cell types. E16 mouse dissociated cortical neurons were cultured for 1 d in vitro (DIV) and immunostained against nestin and DCX. To our surprise, many DCX-positive cells were also positive for nestin (Figure 1A). These DCX/nestin–double positive cells had the morphology of stage 3 immature neurons (using Banker staging; see *Materials and Methods*; Dotti *et al.*, 1988; Figure 1A) and were positive for neuronal-specific βIII-tubulin (see Figure 2D), indicating that they had differentiated into neurons. In addition, GFAP (a marker of astrocytes) was not detected at this early stage of development (unpublished data), in agreement with studies that show that gliogenesis, the formation of astrocytes or oligodendrocytes, does not begin until E17/18 or postnatally, respectively (Miller and Gauthier, 2007). We note that cells lacking neurites were generally nestin-positive and likely correspond to NPCs and some early stage 1 neurons (see Figure 1D). Cells with short processes that might correspond to stage 2 neurons or to nonneuronal cell types had variable nestin expression.

Because nestin is considered a marker of NPCs, we performed a series of rigorous controls to validate the observed staining. We obtained two additional nestin antibodies (raised in chickens [Chk] or goats [Gt]), all against different epitopes in the C-terminal region of nestin. Both antibodies produced immunostaining patterns similar to those for the mouse anti-nestin antibody (Figure 1, A and B). A blocking peptide was available for the goat anti-nestin antibody that allowed testing the specificity of the observed axonal nestin staining. Preincubation of the goat anti-nestin antibody with the immunizing peptide before labeling specifically reduced immunostaining with the goat antibody, but nestin was still detected in distal axons with the mouse anti-nestin antibody in the same cell (Figure 1B). Both of these antibodies appear to be highly specific to nestin, since they detected single bands (~300 kDa) by immunoblot (consistent with the expected size of nestin) in DIV1 E16 cortical mouse neuron lysate (Supplemental Figure S1B).

As an additional validation of antibody specificity, we performed nestin knockdowns with either control nontargeting small interfering RNA (siRNA) (siCon) or a nestin-specific pool of 4 siRNAs (siNes-pool) using Amaxa nucleofection before plating dissociated neurons. GFP was coelectroporated to visualize transfected cells (Figure 1C). Cultures were fixed after 36 h and stained for nestin. The intensity of axonal nestin was then quantified. At 36 h, ~1/3 of GFP-positive stage 3 neurons stained positive for nestin after siCon electroporation, similarly to untransfected cells (see Figure 2C), whereas nestin staining was significantly reduced and essentially undetectable in GFP-positive cells electroporated with siNes-pool (Figure 1C). The specificity of the three nestin antibodies was also assessed by Western blot after siRNA knockdown in neurons (Supplemental Figure S1A). Electroporation is not very efficient in neurons, and the knockdowns were not complete after 36 h, but decreased nestin levels were found after siNes-pool nucleofection for all three antibodies, confirming that the antibodies were specific for nestin. When mouse nestin-myc was transfected into HEK293 cells together with either siCon or siNes-pool siRNA, a near complete loss of nestin signal was observed in the siNes pool–treated condition, while the related intermediate filament vimentin was not affected (Supplemental Figure S1A'). We conclude that nestin protein is indeed expressed in immature neurons in culture. Close reading of the literature revealed that nestin protein has been detected in neurons in humans and mice, both in early differentiating neurons (Cattaneo and McKay, 1990; Messam *et al.*, 1999, 2002; Yan *et al.*, 2001; Walker *et al.*, 2007; Crews *et al.*, 2011), and in subpopulations of adult neurons (Gu *et al.*, 2002; Decimo *et al.*, 2011; Hendrickson *et al.*, 2011; Guo *et al.*, 2014; Liu *et al.*, 2018). Recent advances in single-cell Western blotting have revealed persistent nestin expression in βIII tubulin positive differentiated neural stem cells (Hughes *et al.*, 2014).

Despite the evidence that nestin protein expression is not exclusive to neural stem cells, nestin continues to be used as a specific neural–stem cell marker. We thus performed a side-by-side comparison (Supplemental Figure S1C) of nestin staining in cultures counterstained with the NPC marker Sox2 and the neuronal marker DCX to compare the relative levels of nestin protein. This

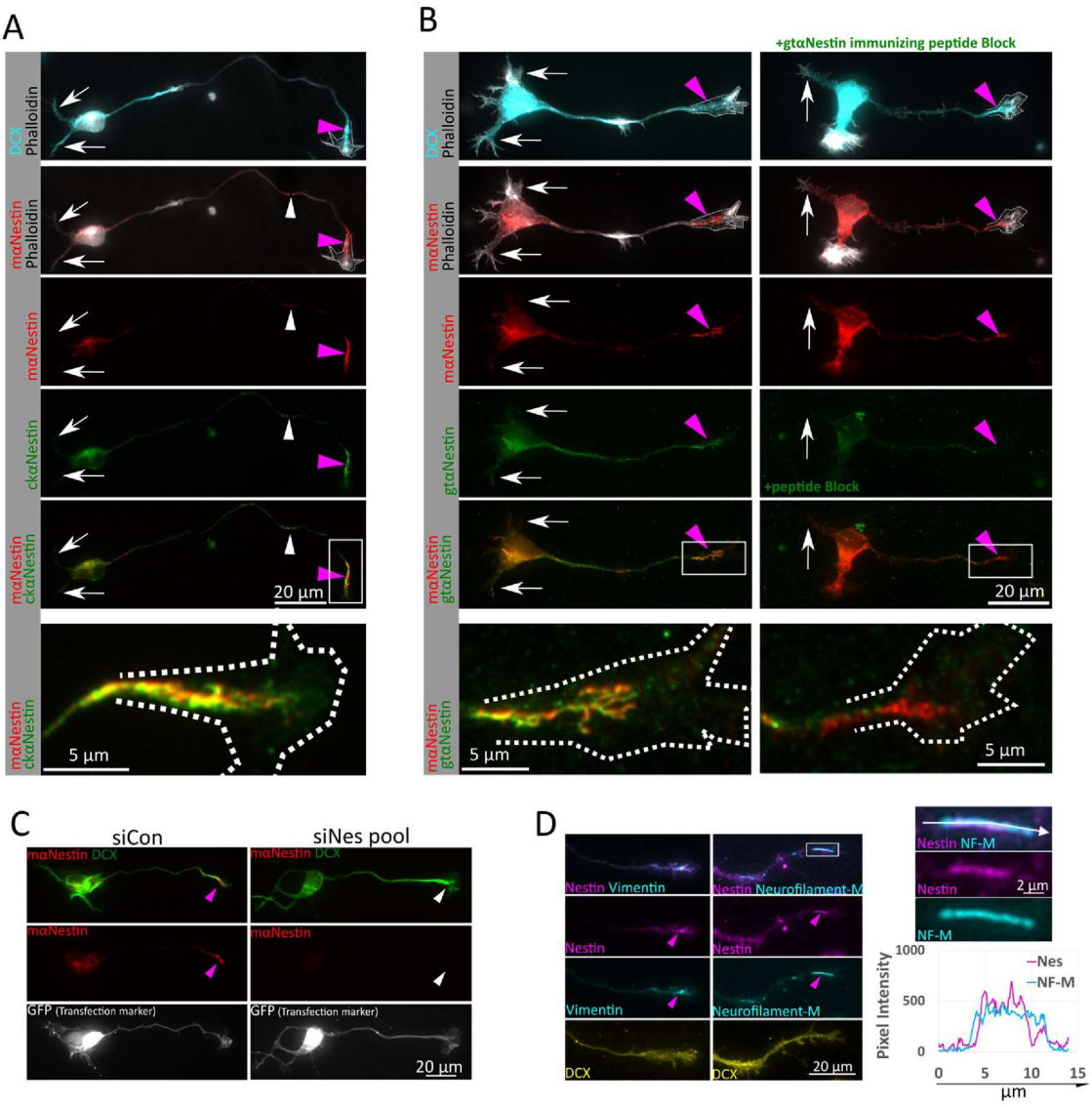

FIGURE 1: Nestin protein expression persists in immature primary cortical neurons in culture. (A). Nestin expression in cultures derived from E16 mouse cortex grown for 1 d (1DIV). Doublecortin (DCX) immunostaining and a stage 3 morphology were used to identify neurons. Nestin is enriched near the axonal growth cone (pink arrowheads), but largely absent from growth cones of minor dendrites (white arrows) using both mouse and chicken anti-nestin antibodies. White arrowheads indicate short nestin intermediate filament segments found along the axon shaft. Bottom panel is enlarged inset of growth cone, rotated, from within the white box. Growth cone outline drown from the phalloidin stain shown in the panels with phalloidin and in the enlargement. (B) Validation of nestin antibody staining on stage 3 neurons with mouse and goat anti-nestin antibodies with immunizing peptide antibody blocking. Both antibodies again show a distal axon enrichment of nestin (pink arrowheads), while the dendrites again are not labeled (white arrows). Preincubation of the goat anti-nestin antibody with the immunizing peptide abolishes all staining, but staining in the distal axons is still detectable with the mouse anti-nestin antibody, which was raised against a different epitope. Shown are E16 mouse cortical neurons 1DIV. Bottom panel is enlarged inset of growth cone from within the white box. Growth cone outline drawn from the phalloidin stain shown in the panels with phalloidin and in the enlargement. (C) Nestin siRNA results in loss of immunostaining, validating that the axonal growth cone staining is due to nestin protein. GFP was cotransfected as a transfection indicator. After 36 h in culture, cells were fixed and immunostained for nestin and DCX. The number of GFP positive cells positive for nestin in the axon as a fraction of the number of cells counted was quantified. (D) Nestin is colocalized with other intermediate filaments in the same assembly group (vimentin and Neurofilament-Medium NF-M) in the distal axons (pink arrowheads) of E16 mouse cortical neurons 1DIV. NF-M expression was low in immature cortical neurons cultured for only 1DIV. High magnification of the boxed region and line scans reveal that nestin and NF-M appear to decorate the same filament structure in partially colocalizing subdomains, as expected for nestin-containing intermediate filaments. Pink arrowheads indicate nestin-positive axonal intermediate filament heteropolymers.

comparison within a single imaging field demonstrates that the nestin protein immunofluorescence level seen in axons (high DCX, but low Sox2 expression) was many times lower than the nestin expression in an NPC cell body (high Sox2, but low DCX expression). High levels of anti-nestin antibody staining were thus confirmed to be a reliable NPC marker when used as a tool to label

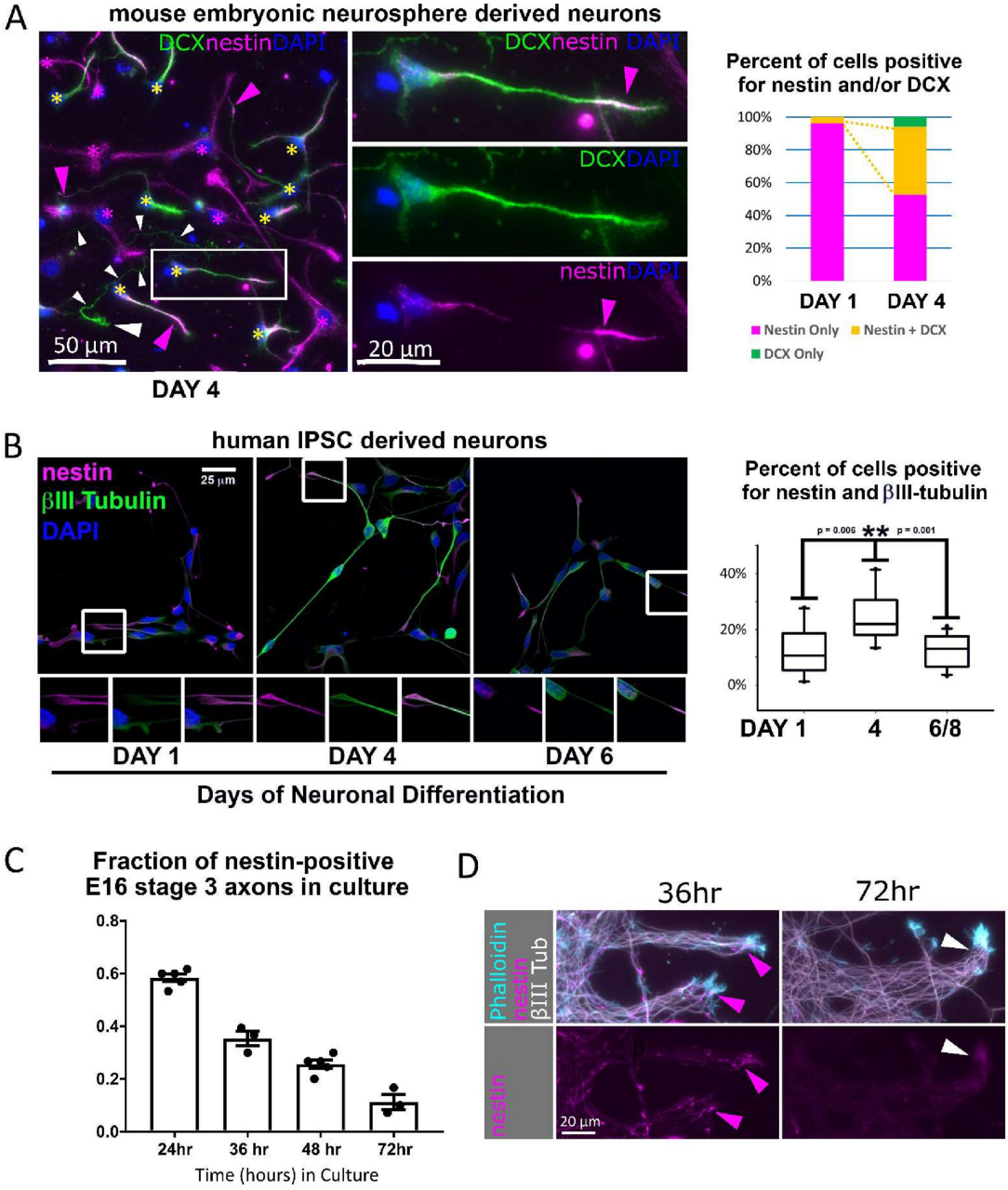

FIGURE 2: Nestin-expressing neurons are observed in multiple rodent and human culture models. (A) Mouse neurosphere NPC cultures: nestin expression was assessed in differentiating dissociated neural progenitor cells (mouse NPC) after 4 d of neuronal differentiation. DCX-positive neurons frequently stain positive for nestin (yellow asterisks), especially in axon tips (pink arrowheads). An example of an axon positive for DCX but not nestin is marked with a series of white arrowheads along the length of the long and thin axon, and a large white arrowhead indicating the growth cone. Nestin–single positive cells are marked with pink asterisks. One example of a double-positive cell is shown in the middle panels to highlight its neuronal morphology and tip-enriched nestin staining (pink arrowhead). The proportion of cells positive for only nestin (red bar) or only DCX (green bar) or double-positive for DCX and nestin (yellow bar) was quantified for NPCs cultured under differentiation conditions from 1 or 4 d. Yellow dotted lines highlight the expanding double positive population (yellow bar). Three hundred twenty-three cells were counted at 1 DIV, and 219 cells at 4 DIV. (B) Human IPSC–derived neuronal cultures: nestin is expressed in human (IPSC) differentiating neurons derived from NPCs in dissociated cultures under differentiating conditions from 1, 4, and 6 d. The distribution of nestin is similar to that in the mouse NPC–derived neurons described above. Percent colocalization with the neuronal-specific βIII tubulin was quantified. A close-up of a nestin-positive axon tip in the boxed region is shown in the panels below the respective images. $n = 14$ (day 1), 10 (day 4), and 14 (day 6–8). (Statistics: Mann–Whitney *t* test). (C) Mouse primary neuron cortical neuron cultures: percentage of nestin-positive neurons decreases rapidly with time in culture (30–60 stage 3 neurons were counted per time point for 3–5 experiments, as shown as the *n*). Cortical neuron cultures were prepared from E16 mice embryos and culture times are indicated. (D) Mouse primary explants: axonal nestin expression is progressively lost between 36 and 72 h in culture. Significant axonal nestin immunostaining is no longer detected by 72 h. E16 mouse cortex was explanted by incomplete dissociation and cultured. Axon fascicles emerging from the explant are shown. Arrowheads point to axon tips.

NPCs and are clearly distinguishable from the lower axonal levels of nestin.

Nestin is present in filaments in distal axons and growth cones

Having validated the nestin antibodies, we next characterized endogenous neuronal nestin distribution. Nestin was not uniformly distributed, but primarily localized to the distal region of the growing axon (pink arrowheads) and was rarely observed in secondary neurites (white arrows; Figure 1A). Variable levels of nestin were often also detected in the cell body. In addition to the distal axon accumulation of nestin, short linear nestin profiles (called squiggles) were often found distributed along the length of the axon (white arrowheads; Figure 1A), which is typical of neurofilaments in young neurons (Benson *et al.*, 1996; Wang *et al.*, 2000). Nestin is an obligate heteropolymer and requires another cytosolic intermediate filament type to assemble into filaments (Steinert *et al.*, 1999). If nestin existed as assembled filaments in neurons, it should be as part of filaments composed of other intermediate filament subunits in addition to nestin. Indeed, we found that nestin colocalized with vimentin, neurofilament-medium (NF-M; Figure 1D), α-internexin (INA), and neurofilament-light (NF-L; unpublished data). Neurofilament-heavy (NF-H) was not detected at these early time points, as NF-H is expressed in more mature neurons (Benson *et al.*, 1996). A magnification inset and a line scan show that nestin and NF-M occupy subdomains within a heteropolymer, as has been demonstrated with nestin filaments in other cell types (Leduc and Manneville, 2017).

In addition to assembled nestin-containing filaments (squiggles) along the axon, we also see nestin staining in the growth cone central domain, which extends more peripherally to various degrees. A typical pattern is represented by the growth cone shown enlarged at the bottom of Figure 1A. Nestin staining appears consolidated at this magnification and resolution. Individual filaments cannot easily be discerned. This staining may represent a tight bundle or tangle of short nestin-containing intermediate filaments (squiggles). In more spread growth cones (such as the growth cone shown enlarged at the bottom left of Figure 1B), nestin staining appears clearly filamentous, suggesting that nestin in neurons can exist at least partially as an assembled heteropolymer filament.

Nestin-expressing neurons are observed in multiple rodent and human culture models

Because neurons are not usually thought to express nestin, we looked at other neuronal models to see whether we observed DCX/nestin–double positive neurons in other contexts. When we prepared neuronal cultures from embryonic rat cortex, we also observed DCX/nestin–double positive neurons (unpublished data). Next, we grew mouse NPCs as neurospheres and then differentiated them into neurons in culture in order to determine whether neurons differentiated from NPCs continued to express nestin. Differentiation into neurons takes several days when this protocol is used. One day after neurosphere dissociation and plating, >95% of cells were nestin-positive, but did not express DCX, consistent with their being NPCs (Figure 2A). The remainder had started to differentiate into neurons and expressed both DCX and nestin. After 4 d of differentiation in dissociated culture, ~50% of cells had differentiated into neurons (DCX-positive). A large proportion of the DCX-positive neurons also expressed nestin. The DCX/nestin–double positive cells had a morphology similar to that of stage 2 or stage 3 cultured primary neurons, and cells with a stage 3 morphology had nestin localized to the tips of neurites (Figure 2A, inset). Only around 10% of cells had no detectable nestin immunopositivity (Figure 2A) and expressed only DCX, consistent with being more differentiated neurons. Differentiating NPCs after 4 d became too crowded to assess on a cell-by-cell basis.

To test whether human neurons similarly express nestin during early differentiation, we assessed nestin expression in cultures derived from human NPCs derived from induced pluripotent stem cells (IPSCs). At 1 d, nestin expression is high and βIII tubulin expression is low, resulting in low colocalization of nestin and βIII tubulin. After 4 d of differentiation, nestin colocalization with βIII tubulin peaked, and nestin staining was clearly detected at the tips of βIII-tubulin positive axons (Figure 2B), confirming nestin expression in cultures of human neurons also. Colocalization again drops at ~1 wk due to decreasing nestin expression: however, nestin is still expressed at the tips of some neurites. To assess whether nestin expression occurred in neurons that are differentiating in a more tissuelike context, we also grew human NPCs as large cortical spheroids, often referred to as "minibrains" (Supplemental Figure S2A). Minibrains recapitulate several developmental processes that are also observed during in vivo development. Nestin staining was clearly detected in neurons (identified by βIII-tubulin expression). Nestin staining was most prominent in neuronal processes with lower βIII-tubulin expression (less mature neurons), while cells expressing higher levels of βIII-tubulin (more mature neurons) were mostly negative for nestin. We conclude that nestin is transiently expressed in both human and rodent neurons and can be observed in a model that recapitulates some aspects of human cortical development.

Nestin protein is transiently expressed broadly among cortical neuron cell types but decreases with maturation

Typical techniques for culturing primary neurons select for cells that recently completed mitosis or are undergoing migration at the time of dissociation (Banker and Cowan, 1977). We thus wondered whether nestin-positive neurons represent a transition state between nestin-positive NPCs and nestin-negative neurons. Alternatively, nestin-positive neurons could be a stable neuronal cell type that maintains nestin expression over longer times in culture. Because cultured cortical neurons maintain cell type fates after dissociation (Romito-DiGiacomo *et al.*, 2007; Digilio *et al.*, 2015), we used two cell type–specific transcription factors to distinguish cortical-projecting (Satb2-positive) from subcortical-projecting (Ctip2-positive) neurons. Nestin expression in DCX-positive neurons did not correlate with either Ctip2 or Satb2 expression (Supplemental Figure S2B). Similarly, when cultures were prepared from E14, E15, or E16 embryos (representing different cortical layer fates), ~2/3 of DCX-positive neurons were nestin-positive after 24 h in culture (unpublished data), regardless of embryonic age at dissection. These data suggest that nestin is expressed by immature neurons of all cortical layers.

Because nestin positiveness was not skewed by neuronal cell type, we next assessed whether nestin expression was correlated with time after differentiation. To this end, we utilized an in vitro time course of neurons dissociated from E16 mouse cortex (Figure 2C), since time in culture represents the maturity of the cell. For the first 12–24 h, around two-thirds of stage 3 neurons expressed nestin in the axon. Plating density had no effect on the percentage of neurons that express nestin (unpublished data). Nestin expression dropped steadily after 24 h, with only one-third remaining nestin-positive at 36 h, one-fourth by 48 h, and less than one-tenth by 72 h (Figure 2C). The change in axonal nestin staining is easily appreciated in axon bundles growing from a cortical explant. At 36 h, nestin expression was clearly seen mostly in the distal region of some axons, but was reduced to near-background levels at 72 h (Figure 2D). These data demonstrate that nestin is expressed transiently in a substantial subpopulation of differentiating cortical

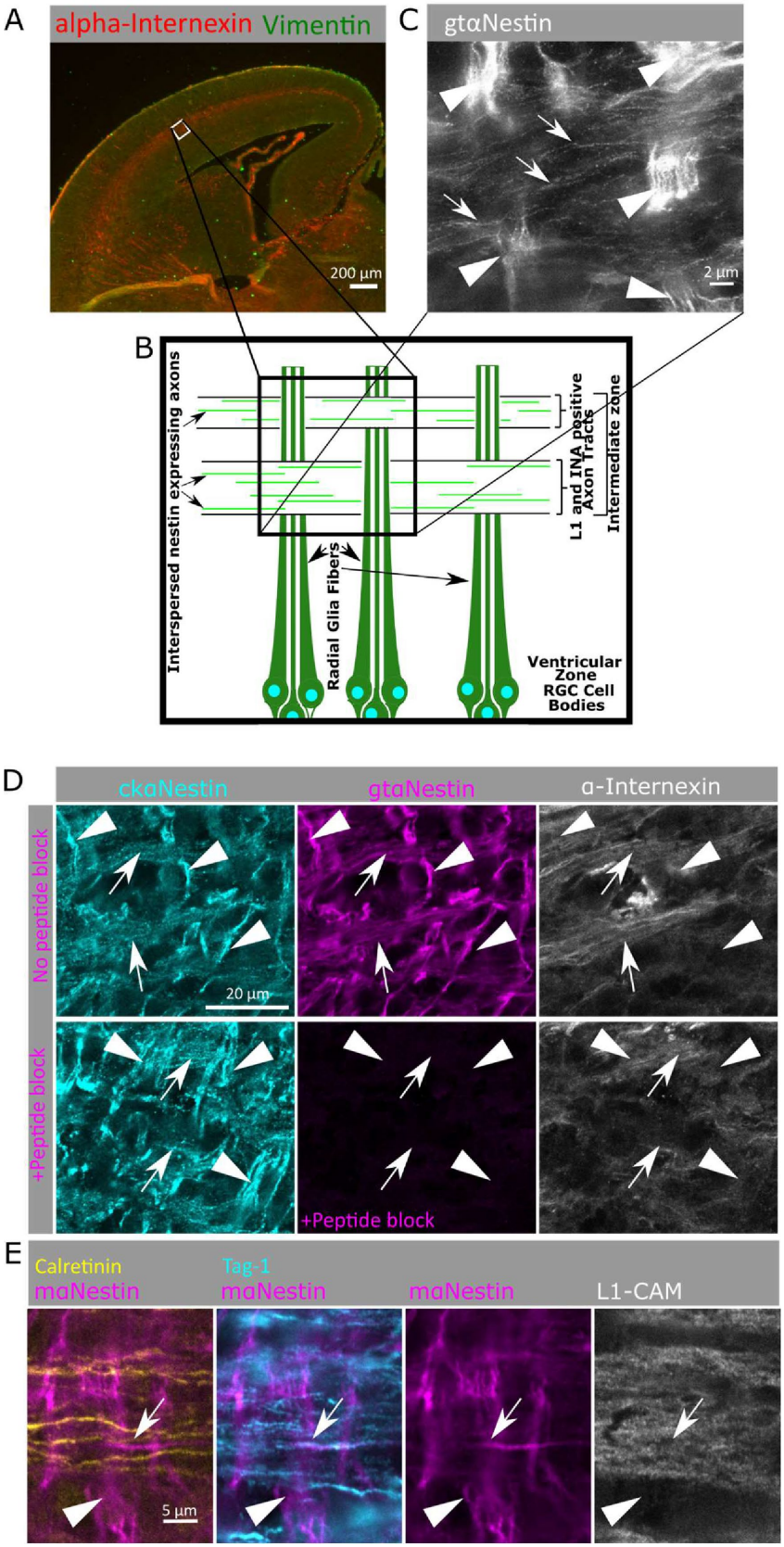

FIGURE 3: Nestin is expressed in subpopulations of cortical axons in developing cortex. (A) A low magnification of a coronal cortical section (E16 mouse) is shown for orientation (top) and showing α-internexin localization to the axon-rich intermediate zone. The white box (lateral lower intermediate zone) is the region imaged in the following panels, and is diagramed below (B), illustrating the vertically oriented radial glia and horizontal IZ axon bundles. (C) Superresolution microscopy (STED) of nestin immunostaining reveals bright staining of radial glial fibers (arrowheads) as well as fainter staining of axons (arrows) in mouse E16 cortex. Many axons in the axon fascicle do not express nestin, so only a subset of axons in the intermediate zone express nestin at this time point. Arrowheads indicate radial glia and arrows indicate nestin-positive axons. (D) Nestin staining of the lower intermediate zone of E16 mouse cortex using chicken anti-nestin (cyan) and goat anti-nestin (magenta) antibodies. Axon tracts are visualized with α-internexin antibody (white). Nestin staining is found in radial glia fibers (arrowheads) as well as in α-internexin-positive axon tracts (arrows). The goat anti-nestin antibody was preincubated with immunizing peptide on sequential cryosections in the lower panels. All staining with the goat anti-nestin antibody was blocked by peptide preincubation, including the axon tract staining, demonstrating that the axon staining was specific and not background staining. All images correspond to higher magnification of the lower intermediate zone of the lateral E16 mouse cortex (boxed regions in A). Radial glia are oriented vertically (arrowheads) and axon tracts are oriented horizontally (arrows). (E) Identification of nestin-positive axons in mouse cortex. The L1-CAM-positive axons (white) contain mixed populations of both cortical and thalamic projections in this brain region. Nestin (magenta) is specifically expressed in axons originating from the cortex (Tag1-positive, cyan), but not in axons with thalamic origin (calretinin-positive, yellow). Arrowheads indicate radial glia, and arrows indicate nestin-positive and Tag1-positive axons.

axons and subsequently down-regulated as differentiation proceeds.

Nestin is expressed in subpopulations of developing cortical neurons in vivo

We next sought to determine whether there was an in vivo correlate to the axonal nestin expression we observed in cultured neurons. Others have shown that developing cortical neurons in the intermediate zone (IZ) consist of a mixture of axons of variable states of maturation—preexisting axon tracts laid down by earlier pioneer neurons, and later born neurons that initiate axon projections during migration through the IZ (Namba *et al.*, 2014). We thus imaged axons in the lower intermediate zone (IZ) of E16 mouse developing cortex, similarly to where nestin mRNA was detected by Dahlstrand *et al.* (1995). In vitro, nestin was not present in all axons and did not fill the whole length of an individual axon. We thus predicted that nestin-positive axons would be detected as a subpopulation of axons in the IZ. We also predicted that axonal nestin would be lower than nestin in NPCs/radial glia.

A low-magnification overview of one hemisphere of the cortex showing vimentin and α-internexin (INA) expression is shown in Figure 3A, along with a schematic to orient the reader. The boxed region in Figure 3A indicates the lateral lower IZ, which is the region in the schematic

imaged in the following panels. All panels in Figure 3, B–E, have the radial glia oriented vertically and the axon tracts oriented horizontally. INA is an intermediate filament expressed early in neuronal development, but not expressed in radial glia (Kaplan *et al.*, 1990; Fliegner *et al.*, 1994; Dahlstrand *et al.*, 1995; Benson *et al.*, 1996). As expected, INA is readily detected in axons of the IZ (Figure 3, A and B). Vimentin is expressed in both radial glia and, at a lower level, neurons (Cochard and Paulin, 1984; Boyne *et al.*, 1996; Yabe *et al.*, 2003; Toth *et al.*, 2008).

As expected, nestin staining intensity in the radial glia (arrowheads in Figure 3, C–E) was high, which made evaluation of nestin staining in axon tracts challenging. However, high-resolution confocal microscopy, the use of distinct axonal markers, and sequential imaging of four channels permitted us to resolve and distinguish between the segregated but interwoven cellular processes of radial glial and IZ axons. Staining with chicken and goat anti-nestin antibodies labeled the bright radial glia fibers (INA-negative) oriented vertically (arrowheads; Figure 3D). Similarly to nestin mRNA (Dahlstrand *et al.*, 1995), INA is present in early cortical axon tracts (arrows), and nestin immunoreactivity was clearly detected in these axon tracts, albeit at lower levels than in radial glia fibers. This staining pattern is similar to what is seen with in vitro axon bundles (Figure 2D). Early defining work had observed low nestin staining on spinal cord axons, but attributed it to background staining by the antibody (Hockfield and McKay, 1985). To assess the specificity of nestin staining on IZ axons, we repeated the peptide-blocking assay used in Figure 1 for the goat anti-nestin antibody on E16 cryosections (Figure 3D). The staining by the goat nestin antibody was completely blocked by preincubation with the immunizing peptide, both on radial glia fibers and on axon tracts, indicating specific staining of nestin on axons in vivo. Both radial glia fibers and axons were still stained with the chicken nestin antibody. In addition, specificity of both the mouse 2q178 antibody and the goat antibody to nestin was assessed by immunoblot of E16 mouse cortex lysate and resulted in clearly labeled single bands that corresponds to the expected size of the nestin protein (Supplemental Figure S1B′). Furthermore, the ~300-kDa band recognized by the goat nestin antibody could be specifically reduced by preincubation with the immunizing peptide, arguing that the observed staining of IZ axons can be attributed to nestin (Supplemental Figure S1B′).

To further characterize the intermediate filament content of the lower IZ axons, costaining for nestin and vimentin was performed (Supplemental Figure S3, A and B). Vimentin was found to have a staining pattern similar to that of nestin, with high levels in radial glia and low levels in axons. The nestin- and vimentin-positive IZ fibers were also positive for the axon marker L1-CAM (Supplemental Figure S3, A and B), confirming their identity as axons. The same axonal nestin staining pattern was seen with the mouse anti-nestin Rat401 monoclonal antibody, the initial antibody used to characterize and define nestin (Hockfield and McKay, 1985; Supplemental Figure S3B). Thus, multiple pieces of evidence demonstrate that nestin is expressed in axons in the IZ at E16 in mouse cortex.

To better visualize the axonal nestin, we performed STED super-resolution microscopy on goat anti-nestin immunostained E16 mouse cortex. The bright nestin-positive radial glia fibers were again the most prominently stained feature, but individual axons with less bright nestin staining could be unambiguously resolved. Nestin is clearly present on a subset of axons of the IZ (Figure 3C*)*. In addition to the axons of cortical neurons (Tag-1 positive) of variable maturity, the IZ contains axons of neurons projecting from the thalamus, calretinin-positive thalamocortical neurons (Shinmyo *et al.*, 2015). We thus used these markers to further define the nestin expressing subpopulations (Figure 3E): L1-CAM for all axons, Tag-1 for cortical axons, and calretinin for thalamocortical axons. Intriguingly, we observed that a subpopulation of cortical (Tag-1 positive) axons had detectable nestin staining, whereas the calretinin-positive (thalamocortical) axons lacked nestin staining (Figure 3E). However, we note that this could be due to differences in the cell type and/or maturity level of cortical vs. thalamic originating axons.

The level of nestin expression in neurons influences growth cone morphology and response to Sema3a

An important question is whether nestin plays a functional role in axons or is simply left over from the mother NPC and no longer plays a role. As a starting point for probing whether nestin still has a function in neurons, we determined whether axons and growth cones were the same or different in neurons with (+) and without (–) nestin (representative images in Figure 4A). We measured axon length, growth cone area, and number of growth cone filopodia (diagram in Supplemental Figure S4F). Nestin levels were not correlated with any variance in axon length (Figure 4E), but interestingly, growth cone area was significantly smaller when nestin was present (Figure 4F). This finding is consistent with previous reports in frog neurons, where the neurons expressing the nestin homolog, tannabin, had smaller blunted growth cones (Hemmati-Brivanlou *et al.*, 1992). How growth cone size is regulated and what effect growth cone size has on growth cone functions is unknown, but other molecules that regulate the actin and microtubule cytoskeleton display a similar phenotype. Growth cone size therefore may be representative of the underlying overall cytoskeletal dynamics, where a more stable cytoskeleton leads to larger growth cones, and a more dynamic cytoskeleton leads to smaller growth cones (Poulain and Sobel, 2007; Khazaei *et al.*, 2014). Others have noted a correlation between axon growth rates and growth cone size; however, our measurements of axon length do not show any significant differences (Argiro *et al.*, 1984; Ren and Suter, 2016).

Because nestin regulates cdk5-dependent processes in muscle cells (Yang *et al.*, 2011), we wondered whether nestin could affect cdk5-dependent processes in neurons as well. Sema3a is upstream of cdk5 in neurons (Sasaki *et al.*, 2002; Ng *et al.*, 2013), and we thus utilized an in vitro bath application "Sema3a collapse assay" to test this idea. In cultured neurons, phosphorylation of cdk5 substrates and morphological changes in growth cones (Dent *et al.*, 2004; Perlini *et al.*, 2015) start within minutes of Sema3a exposure with the loss of growth cone filopodia, resulting ultimately in a collapsed growth cones with no filopodia. Therefore, before complete growth cone collapse, Sema3a leads to retraction of individual filopodia (Dent *et al.*, 2004). Given nestin's role in promoting cdk5 activity at the neuromuscular junction, we hypothesized that growth cone filopodial retraction in response to Sema3a occurred in a nestin-sensitive manner. To quantitatively address this, we counted actin-rich filopodial protrusions of the growth cones (Figure 4G). In untreated cells, filopodia number was inversely correlated to axonal nestin levels (Figure 4G). After a low dose of Sema3a treatment (1 nM for 5 min; Perlini *et al.*, 2015), nestin-positive cells retracted growth cone filopodia significantly, whereas nestin-negative growth cones were not significantly affected by Sema3a during the 5 minute timeframe (shown in Figure 4B, quantified in Figure 4G). The area of the growth cone was not significantly altered in this short time frame as expected (Dent *et al.*, 2004), so we relied on the retraction of filopodia as our most sensitive measurement of Sema3a sensitivity. Because Sema3a is known to act in part through cdk5, we added 10 μM of the cdk inhibitor roscovitine for 30 min before

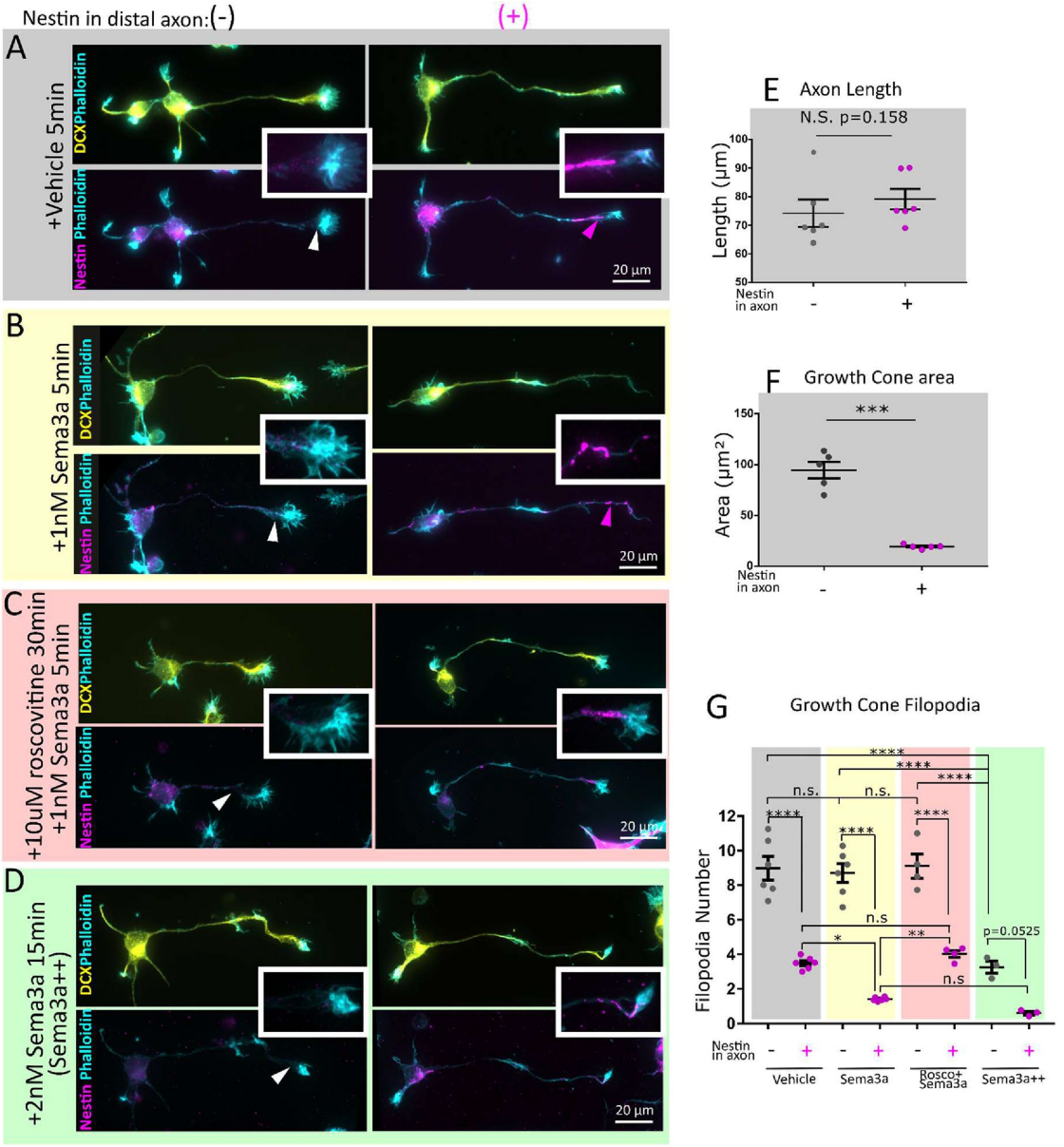

FIGURE 4: Nestin-expressing neurons have smaller growth cones with fewer filopodia and are more sensitive to Sema3a in a cdk5-dependent manner. E16 mouse cortical neurons 1DIV (stage 3) were immunostained against DCX (to confirm neuronal identity), phalloidin (to visualize the growth cones), and nestin. Cells were characterized based on nestin immunoreactivity in the distal axon nestin as Nes(–)—not detected, Nes(+)—nestin-positive. Conditions are untreated (A), 1 nM Sema3a 5 min (B), pretreated with 10 µM Roscovitine 30 min prior to 1 nM Sema3a treatment for 5 min (C), and a Sema3a++ treatment of 2 nM Sema3a for 15 min (D). Insets allow appreciation of the filamentous nature of the nestin immunostaining and proximity to the growth cone. Channel intensity is adjusted equally for nestin and DCX. At low magnification, phalloidin labeling has been adjusted variably to show morphology, but in the insets the phalloidin channel was adjusted in an equal manner. Nestin-expressing neurons are not significantly different by axon length (E), but have significantly smaller axon growth cones (F). Neuron morphology was quantified (30–40 cells per independent experiment). Mean of each experiment and SEM are indicated. Statistical test was a *t* test with $n = 6$ (E) or $n = 5$ (F). (G) Neurons with nestin have fewer filopodia than those without nestin. In cells treated with 1 nM Sema3a for 5 min, the nestin-positive cells had a significant reduction in filopodia in comparison with untreated nestin-positive cells, whereas the nestin-negative cells did not. Conditions have been color coded for ease of comparison. Roscovitine inhibited the decrease in filopodia number after Sema3a treatment. When a high dose (2 nM) and longer treatment (15 min) of Sema3a are used, both nestin-negative and -positive neurons retract filopodia and significantly so, indicating that nestin is not absolutely required for Sema3a-induced filopodial retraction, but increases Sema3a sensitivity. Filopodia number was quantified for 6 (vehicle, Sema3a), 4 (roscovitine + Sema3a), or 3 (Sema3a++) independent experiments. An average of 30–40 cells quantified per experiment is shown. Mean of each experiment and SEM are indicated. Normality was confirmed with the Shapiro–Wilk normality test. Statistical test was one-way ANOVA with Tukey's multiple comparison correction, with n = number of experiments. Each condition was compared with every other condition.

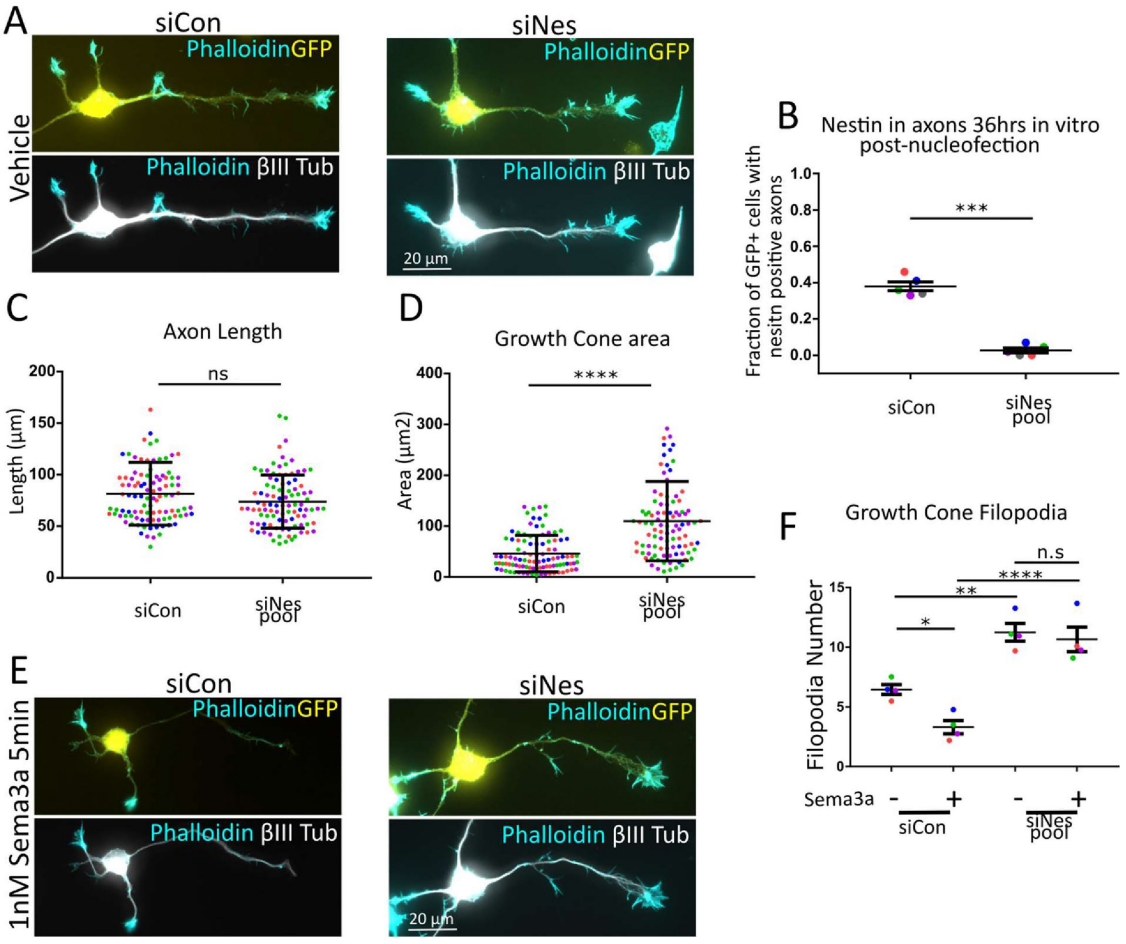

FIGURE 5: Nestin siRNA results in abnormal growth cone morphology and resistance to Sema3a. Representative images of primary E16 mouse cortical neurons that were cotransfected with a plasmid encoding GFP and either control siRNA (siCon) or nestin siRNA (siNes) and cultured for 36 h. GFP booster was used to visualize transfected cells, Tuj1 (βIII-tubulin) was used to confirm neuronal identity and for cell morphology, and phalloidin to visualize growth cones (A, E). The efficiency of nestin knockdown was quantified (B) by counting GFP (transfected) and nestin-positive cells by immunostaining in stage 3 neurons. Approximately one-third of siCon neurons express nestin at 36 h in the axon. Very few transfected neurons showed nestin expression in the axon under siNes conditions. 120-140 cells per condition were counted in $n = 5$ independent experiments. $p < 0.001$ (paired t test). In vehicle-treated conditions (A), siNes treated cells had no significant difference in axon length (C) but resulted in significantly larger growth cones (D). $n = \sim 100$ cells (plotted on the graph) were measured for each condition and significance was measured by an unpaired Mann–Whitney rank comparison test. A Shapiro–Wilk normality test indicated that the data were not normal. A t test was also performed (to be consistent with other analyses) for the growth cone area data separately with each experimental average, $n = 4$ (each a different color on graphs), and resulted in a significant p value of 0.025. siCon- or siNes-transfected neurons were treated for 5 min with 1 nM Sema3a (E). siNes resulted in more filopodia per growth cone, and these filopodia were resistant to Sema3a retraction (F). Approximately one hundred cells in four independent experiments were averaged and $n = 4$ was used for statistical analysis (one-way ANOVA with Sidak correction—only the pairs shown were compared). Normality was confirmed with the Shapiro–Wilk normality test.

Sema3a application. Roscovitine pretreatment inhibited the decrease in filopodia number after Sema3a treatment (Figure 4, C and G). Roscovitine inhibits cdk5 potently, but it also inhibits some of the mitotic cdks (cdk2 and cdc2), albeit less effectively. Because neurons are postmitotic, they have few to none of the mitotic cdk activities. It is thus likely that the roscovitine inhibition of the Sema3a effect is due to cdk5 inhibition.

Last, nestin is not absolutely required for Sema3a sensitivity, since higher and longer Sema3a stimulation (2 nM for 15 min) resulted in filopodial retraction even in nestin-negative cells (Figure 4, D and G). Together these data demonstrate a strong correlation between axonal nestin expression and growth cone size, and Sema3a-mediated filopodial retraction.

Nestin depletion results in abnormal growth cone morphology and decreased sensitivity to Sema3a

To test for nestin-dependent sensitivity to Sema3a directly, we used nestin siRNAs to deplete nestin protein from neurons and assess growth cone morphology and response to Sema3a. Neurons electroporated with the siNes-pool and GFP (to visualize transfected cells; Figures 1C and 5, A and E; Supplemental Figure S1A) were analyzed for differences in morphology. Neurons that received the siNes pool had no variance in axon length (Figure 5C) but had large growth cones (Figure 5D) and more growth cone filopodia (Figure 5F) than siCon, mirroring the effects seen from analysis of endogenous variation of nestin expression (Figure 4). To confirm that this effect was specific to nestin depletion and not an off-target effect,

the four siRNAs that make up the siNes-pool were tested individually. Two of them (#1 and #17) were effective both for depleting nestin and for increasing growth cone size and filopodial number (Supplemental Figure S4, A–E). More than one distinct siNes thus resulted in the same phenotype as the siNes pool, consistent with specificity of the phenotype to nestin depletion. Consistent with this conclusion, siNes #4 failed to reduce nestin levels and did not affect growth cone morphology, similarly to siCon (Supplemental Figure S4, A–E).

As expected, siCon-transfected neurons had a significant reduction in filopodia number following 1 nM Sema3a treatment for 5 min. Neurons transfected with the siNes pool and then treated with Sema3a (1 nM 5 min), in contrast, showed no change in filopodia number (Figure 5E), and they were thus insensitive to this dose of Sema3a. These results demonstrate, surprisingly, that nestin increases the sensitivity of axonal growth cones to Sema3a.

DISCUSSION

Neural development requires that axonal growth cones respond to a variety of extracellular guidance cues to change their direction of growth for proper wiring of the nervous system (Kolodkin and Tessier-Lavigne, 2011). Importantly, not all growth cones traversing the same environment respond the same way to the same cues at the same time (Mintz *et al.*, 2008; Carcea *et al.*, 2010; Wang *et al.*, 2014). Even more remarkably, the same growth cone often responds differently to the same axon-guidance cue when encountering it at a different point in time and space (Kolodkin and Tessier-Lavigne, 2011). As an axon grows into new brain regions, it must therefore respond not only to new cues, but often differently to the same, previously encountered cue. The molecular mechanisms underlying this variable response to the same cue are poorly understood. We propose that nestin acts as a sensitizer and might provide a gain control mechanism, such that axons lacking nestin are less repelled by Sema3a than axons expressing nestin.

Nestin is highly expressed in NPCs, but expression persists in young neurons

We made the surprising discovery that nestin, the most commonly used marker for NPCs, is also found in young neurons. Our conclusion that nestin is in fact expressed in neurons is based on multiple lines of evidence, including multiple antibodies to distinct epitopes, multiple distinct siRNAs to knockdown expression, and peptide blocking of nestin immunostaining.

We find that nestin localizes predominantly to the distal axon and is not found enriched at dendritic tips. This is an intriguing observation, given the importance of neuronal polarity (Takano *et al.*, 2015) and of the opposite growth directions of the future axons and apical dendrite in early cortical neurons (Polleux *et al.*, 2000; Wang *et al.*, 2014). In the distal axon, nestin is found in tightly bundled filaments that codistribute with other neuronal intermediate filaments at the wrist region of the growth cone, but individual nestin filaments can also be seen to extend into the central region of the growth cone and even sometimes into the periphery. Nestin is thus well positioned to regulate growth cone dynamics.

A remaining question is whether the nestin protein detected in neurons is a remnant that was translated when the cell was an NPC, or is made from nestin mRNA in neurons. Our ability to knock down nestin with siRNA following dissociation suggests that nestin mRNA is present after dissociation and actively translated in early neurons. Several papers have described nestin mRNA in neurons in developmental, normal adult, and pathological/injury contexts (Crino and Eberwine, 1996; Kuo *et al.*, 2005; Zhu *et al.*, 2011; Perry *et al.*, 2012; Arner *et al.*, 2015; Bigler *et al.*, 2017; Dey *et al.*, 2017; Farzanehfar *et al.*, 2017a,b). Nestin expression is thus not excluded from neurons. Nestin's presence in subpopulations of adult neurons suggests that some neurons may never lose nestin expression or may regain it later. The best evidence for nestin mRNA in early postmitotic cortical neurons arises from a single cell RNA-seq experiment in which flash tag labeling was used to birthdate newborn cells in the cortex of an E14 mouse embryo in utero, followed by dissociation and single-cell RNA-seq 6–48 h after labeling (Telley *et al.*, 2016). This unbiased single-cell approach in vivo revealed that nestin mRNA does persist in some newborn neurons of the embryonic mouse cortex 24–48 h after cell division. This suggests that early neurons continue to make new nestin. We propose that newly made neuronal nestin still plays a functional role. Furthermore, the initial nestin mRNA localization study did detect nestin mRNA in the intermediate zone (Dahlstrand *et al.*, 1995), where early axons are located.

A role for neuronal nestin in vivo?

Little is known about nestin function in the developing brain overall, and existing reports of nestin phenotypes are conflicting. A number of defects have been reported for nestin knockdown in neural stem cells in culture, including increased cell death, but proliferation and differentiation were reportedly normal (Di *et al.*, 2014; Hu *et al.*, 2016). Down-regulation of nestin also augmented sensitivity to oxidative stress (Sahlgren *et al.*, 2006), implicating nestin in cellular stress pathways. In zebrafish, microcephaly and small eyes were reported after knockdown of nestin expression with morpholinos (Chen *et al.*, 2010). Again, NPC cell death was increased. There were also some defects in axon tracts, but it was not clear whether these were a consequence of NPC phenotypes or independently arising in neurons. Another paper used in utero electroporation of shNestin into rat embryos and found fewer migratory neurons (Xue and Yuan, 2010). This was reported to be due to cell cycle arrest of NPCs in the G1 phase of the cell cycle. Cell death was not increased. The shNestin phenotype could be rescued with WT nestin (Xue and Yuan, 2010). The same year, the first mouse nestin KO papers were published. One paper reported embryonic lethality with severe brain defects due to increased NPC cell death (Park *et al.*, 2010). The reported phenotype thus appeared similar to the zebrafish phenotype and possibly also to the rat shNes phenotype. A second nestin KO paper, in contrast, reported viable and fertile mice showing only mild motor deficits (Mohseni *et al.*, 2011). The motor deficits were traced to defects in myoblasts, resulting in abnormal NMJ formation with impaired AChR clustering. Adult (but not embryonic) neurogenesis was found to be impaired in the viable nestin KO strain by a surprising non–cell autonomous mechanism where nestin-expressing astrocytes regulate Notch signaling in progenitors to maintain stemness (Wilhelmsson *et al.*, 2019). In addition, some behavioral defects were described in the same paper, in particular with respect to long-term memory in an object recognition test (Wilhelmsson *et al.*, 2019). A role for nestin in maintaining NPC pools is thus likely, but data are contradictory and controversial. Furthermore, the mechanism by which nestin might regulate embryonic NPC pools is not known.

A role for nestin in neurons during embryonic development is completely unknown. We provide evidence that nestin modulates responsiveness to Sema3a in cultured cortical neurons. What role could the neuronal nestin play in vivo? At these early developmental time points, Sema3a is important for initial axon positioning and fasciculation (Beher *et al.*, 1996; Zhou *et al.*, 2013). Because Sema3a exists in vivo as a gradient emanating from the ventricular zone and

cortical plate, it is conceivable that nestin-mediated Sema3a sensitivity could dictate the position of the axon within the IZ (Ruediger *et al.*, 2013). We were unable to deplete nestin in vivo acutely, because nestin depletion by in utero short hairpin RNA electroporation results in loss of migratory neurons in the cortex. Because nestin expression is much higher in NPCs, the authors conclude that this phenotype is likely due to impaired cell division of NPCs (Xue and Yuan, 2010), precluding analysis of nestin function in postmitotic neurons. More detailed analysis of the nestin-positive axons in vivo will be needed to predict more precisely what guidance defects might be found if neuronal nestin expression were disrupted. Given our results, this is something of great interest to do in the future, but a conditional KO might be needed to avoid depleting nestin in NPCs in order to separate any effects of nestin in NPCs from those in early neurons.

Nestin as a novel gain control element in Sema3a signaling

Several other molecules have been shown to modulate responsiveness to guidance cues (Kaplan *et al.*, 2014), including coreceptors (Dang *et al.*, 2013), lipid raft components (Carcea *et al.*, 2010), second messengers (such as cAMP/cGMP and calcium; Henley *et al.*, 2004; Shelly *et al.*, 2011; Tojima *et al.*, 2014), and modification of downstream signaling cascades by ERM (Mintz *et al.*, 2008), α2-chimaerin (Brown *et al.*, 2004; Ip *et al.*, 2011), and 14-3-3 proteins (Kent *et al.*, 2010; Yam *et al.*, 2012). Our results now add the intermediate filament protein nestin to this category of proteins that can variably regulate responsiveness to Sema3a. The previously identified modulators often serve to vary the degree of signaling output to alter the cytoskeleton and adhesive properties of the growth cone (Vitriol and Zheng, 2012; Wang *et al.*, 2014). Nestin might similarly modulate cytoskeletal responses to Sema3a, but the molecular mechanism is currently not known. Multiple cytoskeletal proteins are known substrates for cdk5 and act downstream of Sema3a. They are obvious candidates for being nestin effectors in this cascade and mediating the increased Sema3a sensitivity of nestin-expressing neurons. Studies on the role of nestin in cancer cells has demonstrated the importance of nestin for migration/invasion, proliferation, and survival of cancer cells—which are reduced after nestin depletion by altering cell signaling pathways (Wei *et al.*, 2008; Hyder *et al.*, 2014; Narita *et al.*, 2014; Zhao *et al.*, 2014; Liang *et al.*, 2015; Zhang *et al.*, 2017). How nestin promotes higher sensitivity to low doses of Sema3a remains unknown, and future investigation will assess how phosphorylation of cdk5 substrates is affected by the presence or absence of nestin.

One other remaining question is how nestin, which is primarily localized to the distal parts of the axon and to the central domain and/or wrist of the growth cone, affects the stability and dynamics of peripherally localized filopodia. Other examples of proteins initially described as being wrist-localized have been found to affect filopodial morphology, but it is an open question how actin-based structures and microtubule networks coordinate growth cone morphology and axon growth (Grabham *et al.*, 2007; Astle *et al.*, 2011). In fact, intermediate filaments are known to cross-link and interact with these other cytoskeletal elements (Chang and Goldman, 2004). Nestin might similarly affect the other structures of the growth cone by structural or regulatory cross-talk. This is currently not known, but is an exciting future direction for further research.

In summary, we have identified nestin intermediate filament protein at the axonal growth cone, where it plays a role in regulating growth cone morphology. In addition, we have identified nestin as a novel downstream effector of Sema3a signaling. Nestin intermediate filament protein could thus play critical regulatory roles in axon guidance responses by serving as a "gain control" element to increase responsiveness of a subset of axons to a common guidance cue.

MATERIALS AND METHODS

Antibodies

Mouse anti-nestin Rat401: Recognizes the unique C-terminal tail region of nestin (Su *et al.*, 2013). All experiments shown with 2q178 were also repeated with this antibody. Note that this antibody and the other antibodies recognize full-length nestin. 1:200 IF, 1:500 IHC, 1:500 WB. DSHB Cat.# Rat-401; also rat-401 RRID:AB_2235915'

Mouse anti-nestin 2q178: This clone and RAT401 produce indistinguishable staining patterns. All staining and blotting were done with this antibody unless otherwise noted. 1:200 IF, 1:500 IHC, 1:500 WB. Santa Cruz Biotechnology Cat.# sc-58813; RRID:AB_784786.

Goat anti-nestin R-20: Raised against peptide in the unique C-terminal tail region of nestin. 1:500 IF, 1:200 IHC. Santa Cruz Biotechnology Cat.# sc-21249; RRID:AB_2267112.

Chicken anti-nestin: Three peptide-directed antibodies combined with the unique C-terminal tail region of nestin. 1:300 IF, 1:400 IHC, 1:3000 WB. Aves Labs Cat.# NES RRID:AB_2314882.

Rabbit anti-nestin AB92391: Raised against peptide in the unique C-terminal tail region of nestin. 1:500 IF. Abcam Cat.# ab92391; RRID:AB_10561437.

Rabbit anti-DCX: 1:1200 IF, IHC, 1:4000 WB. Abcam Cat.# ab18723; RRID:AB_732011.

Mouse anti-βIII tubulin Tuj1: 1:800 IF. A generous gift from the Deppman Lab, University of Virginia (UVA), A. Frankfurter, UVA Department of Biology. Cat.# TuJ1 (beta III tubulin); RRID:AB_2315517.

Chicken anti-βIII tubulin: 1:200 IF. Aves Labs Cat.# TUJ RRID:AB_2313564.

Rat anti α-tubulin: 1:2000 WB. Santa Cruz Biotechnology Cat.# sc-53030; RRID:AB_2272440.

Rabbit anti-vimentin: 1:100 IF, 1:100 IHC, 1:1000 WB. Bioss Cat.# bs-0756R; RRID:AB_10855343.

Rat anti-Myc tag 9E1: 1:1000 WB. ChromoTek Cat.# 9e1-100; RRID:AB_2631398.

Mouse anti-neurofilamentM 2H3: 1:200 IF. DSHB Cat.# 2H3; RRID:AB_531793.

Mouse anti-αinternexin 2E3: 1:100 IHC. Sigma-Aldrich Cat.# I0282; RRID:AB_477086.

Rat anti-L1: 1:150 IHC. Millipore Cat.# MAB5272; RRID:AB_2133200.

Mouse anti-Tag1-4D7 (DSHB): 1:150 IHC. DSHB Cat.# 4D7; RRID:AB_2315433.

Rabbit anti-calretinin: 1:600 IHC. Millipore (Chemicon) Cat.# PC254L-100UL; RRID:AB_564321.

Goat anti-Sox2: 1:250 IF. Santa Cruz Biotechnology Cat.# sc-17320; RRID:AB_2286684.

Rat anti-CTIP2: 1:400 IF. BioLegend Cat.# 650601; RRID:AB_10896795.

Rabbit anti-SatB2: 1:400 IF. Abcam Cat.# ab92446; RRID:AB_10563678.

GFP booster nanobody: 1:600 IF. ChromoTek Cat.# gba488-100; RRID:AB_2631434.

Phalloidin 568: 1:150 Invitrogen.

Neuronal culture

Primary cultures of cortical neurons were obtained from embryonic day 16 (E16) mouse cortex of either sex as described. The protocol follows institutional animal care and use committee (ACUC) protocols (approved animal protocol #3422). Cells were plated on poly-L-lysine coverslips and incubated with DMEM with 10% fetal bovine serum (FBS). After 8 h, the cells were transferred into serum-free medium supplemented with B27 (Invitrogen) and glutamine and

cultured for a total of the indicated time periods in vitro (DIV). Cells were plated at ~100,000 cells per 15-mm coverslip, or at 50,000 in the low-density experiment, or 125,000/coverslip in electroporation experiments. Cortical neurons for culture were harvested at E16 before gliogenesis. Thus nonneuronal glia are rare in these cultures, but occasional nestin/Sox2-positive, GFAP-negative persisting neural stem cells were found.

Two-dimensional explants were acquired from E16 cortex, but only partially dissociated before plating as described above.

Cells for Sema3a treatment assay were prepared as described above. At 24 or 36 h, cells were treated with mouse Sema3a (R&D Systems) diluted in growth media for 5 min at 1 nM or 15 min at 2 nM as indicated before fixation. In some experiments, cells were pretreated with 10 µM Roscovitine (Cayman Chemical) for 30 min before Sema3a treatment. Time course experiments were fixed at the indicated time points after plating.

Immunofluorescence

Cells were fixed in 4% paraformaldehyde–PHEM–sucrose (PPS: 60 mM PIPES, 25 mM HEPES, 10 mM EGTA, 2 mM $MgCl_2$ [PHEM], 0.12 M sucrose, 4% paraformaldehyde, pH 7.4) for preservation of the cytoskeleton and cellular morphology with prewarmed fixative and fixed at 37°C for 20 min. Thorough permeabilization was required for nestin/intermediate filament visualization in neurons. Coverslips were permeabilized with 0.4% Triton X-200 in 1% BSA/PBS for 20 min for nestin and intermediate filament staining, or 0.2% Triton-X when no intermediate filaments were being immunostained, and then blocked for 30 min in 10% BSA, 5% normal donkey serum (NDS) in phosphate-buffered saline (PBS). Primary antibodies were diluted in 1% BSA in PBS, and secondary antibodies in 1% BSA, 0.5% NDS in PBS. Primary antibodies were incubated overnight at 4°C, and secondary antibodies for 90 min at room temperature. Appropriate species-specific Alexa-350-, -488-, -568-, or -647-labeled secondary antibodies raised in donkey (Invitrogen) were used for fluorescent labeling. Phalloidin-568 (Invitrogen) at 1:150 was used to visualize F-actin and DAPI to visualize nuclei. For peptide-blocking negative control experiments, the goat anti-nestin antibody was diluted at 1:500 with the corresponding immunizing peptide (Santa Cruz) at 1:50 and incubated at room temperature for 3 h. The goat anti-nestin antibody for the nonblocked condition was diluted and incubated similarly, but in the absence of peptide. Coverslips were mounted with ProLong Gold (Invitrogen) and imaged with a Zeiss Z1-Observer with a 40× (for population counting) or 63× (for morphology analysis) objective. Images were captured with an Axiocam503 camera using Zen software (Zeiss) and processed identically within experiments. No nonlinear image adjustments were performed.

Histology

Human IPSC–derived cortical organoids (minibrains) or embryonic E16 mouse brain were dissected and placed in 4% PFA and 6% sucrose in PBS at 4°C overnight. Tissue was then cryoprotected by sinking overnight in 30% sucrose. Tissue was imbedded in OCT, and brains were cut by coronal cryosection into 16-µm sections (Zeiss confocal imaging) or 10-µm sections (Abberior superresolution). Sections were mounted directly on slides, permeabilized with 3% NDS + 0.2% Triton X-100 in PBS for 1 h, and blocked with 10% BSA for 30 min. Indicated primary antibodies were diluted in permeabilization buffer overnight at 4°C, and secondary antibodies 2 h at room temperature following thorough washing with PBS. Sections were mounted with Prolong Gold. For peptide-blocking negative control experiments, the goat anti-nestin antibody was diluted at 1:100 with the corresponding immunizing peptide (Santa Cruz) at 1:10 and incubated at room temperature for 3 h. The goat anti-nestin antibody for the nonblocked condition was diluted and incubated similarly, but in the absence of peptide. The antibody was then used as described above. Of note, the anti-Tag1 IgM antibody has a cross-reaction with mouse immunoglobulin G (IgG) secondary antibodies, so staining with mouse IgG and mouse IgM antibodies was done sequentially. Confocal imaging of cryosections was carried out on an inverted Zeiss LSM880 confocal microscope using a 63× objective. Superresolution STED imaging utilized an Abberior STED confocal with 100× objective at the Keck Microscopy Center (UVA). A donkey anti–goat-488 (Invitrogen) secondary antibody was imaged using a 595-nm extinction laser.

Neuron nucleofection

After cells were dissociated from cortex, but before plating, they were electroporated by Amaxa 4d nucleofection according to the manufacturer's protocols. Eight hundred thousand cells were electroporated in small-volume (20-µl) cuvettes using P3 primary cell solution and EM-100, CL-133, and CU-100 programs variably between experiments. All three of these programs worked similarly in our hands. GFP plasmid (pCMV-GFP-Clonetech; 0.1µg) was used as a transfection marker, together with 100 nM siRNA (siCON-SCBT sc-37007, siNes smart-pool Dharmacon siGenome M-057300-01-0010, consisting of four individual siRNAs [D-057300 -01,-03,-04, and -17] with target sequences siRNA #1- AAAGGUG-GAUCCAGGUUA, siRNA #3 D-AGACAAGACUCAUGAGUC, siRNA #4 CAGCAGGCAUUUAGACUUC, siRNA #17 GCGACAAC-CUUGCCGAAGA). All four target the region in the mRNA corresponding to the unique C-terminal tail of nestin protein, which is unlike other intermediate filaments.

Molecular biology

Circular mouse nestin cDNA was obtained as a gift from Bruce Lahn (University of Chicago). Briefly, PCR was used to generate *Eco*R1 and *Hin*dII sites on the 5′ or 3″ end, respectively, of full-length mouse nestin. Both the insert and vector were treated with *Eco*R1 and *Hin*dII. The cut insert was ligated into pCDNA3.1 Myc-His(+) B.

Cell culture and transfection

HEK293 cells were maintained in DMEM + 10% FBS, and all transfections were conducted using Lipofectamine 2000 (Invitrogen) according to the manufacturer's protocol. mNestin-myc and respective control or nestin siRNAs were transfected simultaneously according to the recommended instructions.

Western blot

Cells were washed with ice-cold PBS and lysed directly on the plate (6 cm) into lysis buffer (400 µl; 50 mM Tris HCl, 150 mM NaCl, 1% NP-40, 1 mM EDTA, 1 mM dithiothreitol [DTT], 1 mM phenylmethylsulfonyl fluoride [PMSF], 1× HALT protease/phosphatase inhibitor cocktail). After rotisserie of lysates at 4°C for 30 min, lysates were cleared by centrifugation at 21,000 × *g* for 15 min at 4°C. Supernatants were diluted with 5× Laemmli buffer and equivalent amounts were run on a 4–20% polyacrylamide gel. After transfer onto nitrocellulose with the BioRad Transblot, the membrane was blocked with Licor TBS blocking buffer for 1 h at room temperature. Primary and secondary antibodies were diluted in 50% blocking buffer, 50% PBS, 0.1% Tween-20. Peptide blockage was performed on diluted primaries in blocking buffer for 8 h at room temperature with a 10× excess of peptide to

antibody ratio before incubation with blots. Primary antibodies were incubated overnight at 4°C, followed by near-infrared secondary antibodies for 1 h at room temperature. Blots were imaged with a Licor Odyssey CLx imager.

Image analysis

ImageJ was used for all image analysis.

Neuron morphology and nestin expression analysis

Neuron staging was performed according to the Banker neuron staging method, and neurites were designated as axons if they were 2× longer than the next longest neurite (dendrites). Nestin positiveness in the axons of neurons was assessed by outlining the distal region of the axon and measuring the maximum nestin immunostaining in the region. If this value was at least 1.5× average background, then a cell was considered positive for nestin. In siRNA experiments, only green GFP+ (transfection indicator) cells were imaged and counted for both morphology and nestin siRNA efficiency analysis. All counts were confirmed by blind analysis. How morphology measurements were made is depicted in Supplemental Figure S4F.

Filopodial protrusions were counted using the phalloidin channel, and any actin-rich protrusion from the growth cone was counted.

Axon length was the length of the axon from the cell body to the growth cone tip.

Growth cone area and perimeter were assessed by measuring traced outlines of the growth cone, not counting the filopodial protrusions, and extending down to the point where the splayed growth cone microtubules consolidated into bundles in the axon shaft.

Mouse neural stem cell marker expression was assessed by manually counting DCX-, nestin-, and DAPI-stained differentiated neural stem cells for immunopositivity above background levels in any part of the cells.

Human IPSC nestin and βIII tubulin colocalization was assessed per image using the ImageJ colocalization plug-in.

Mouse neural stem cell culture

Embryonic (E16) cortical neural stem cells were prepared as described by Pacey *et al.* (2006) and grown as neurospheres for at least three passages to ensure purity before use for dissociated and differentiating cell experiments. For these experiments, neurospheres were dissociated using a stem cell chemical dissociation kit, plated in poly-L-lysine–coated coverslips for 1 d, and fixed and immunostained as described. For 4DIV, proliferative medium was replaced with media lacking EGF and FGF growth factors until 4 DIV, fixed, and processed for immunostaining as described.

Neural differentiation of human induced pluripotent stem cells

Human induced pluripotent stem cells from neurotypic control 9319 were generated by Kristen Brennand in the laboratory of Fred Gage (Salk Institute). NPCs were generated through an embryoid body protocol as described by Brennand *et al.* (2011). For neuronal differentiation, we plated 75,000 control NPCs on each poly-ornithine- and laminin-coated 18-mm glass coverslip. After 24 h, cells were switched to neuronal differentiation media consisting of DMEM F12 + Glutamax and supplemented with N2 and B27 with retinoic acid and 20 ng/ml BDNF, 20 ng/ml GDNF, 400 μM cyclic AMP, and 200 nM ascorbic acid. Half of the medium was replaced with fresh medium every 3 d. Neurons were fixed with 4% formaldehyde with 4% sucrose on the days indicated and used for subsequent immunofluorescence analysis.

Generation of cortical organoids

Human fibroblasts from neurotypic control 7545 were obtained from the Coriell Institute and reprogrammed into induced pluripotent stem cells by the laboratory of Mike McConnell (UVA) using a CytoTune Reprogramming Kit (Life Technologies) and maintained in Essential 8 media (Life Technologies). Cortical organoids were grown using a low-attachment protocol. Briefly, we used dispase to detach hIPSC colonies from matrigel dishes. These colonies were placed in ES/DMEM medium (GlobalStem) supplemented with 20% Knockout Serum Replacement (Life Technologies) and treated with 5 mM Dorsomorphin and 10 mM SB-431542 for the first 5 d. The ROCK inhibitor Y-27632 (10 mm) was added for the first 48 h. From day 6 to day 24, spheroids were fed with neuronal medium consisting of Neurobasal A with B27 without vitamin A, GlutaMax, and penicillin/streptomycin (Life Technologies) and supplemented with 20 ng/ml EGF and FGF2 (Peprotech). From day 25 to day 42, the growth factors were replaced with 20 ng/ml BDNF and NT3 (Peprotech). From day 43 onward, BDNF and NT3 were removed and organoids were grown solely in neuronal medium.

Statistical analysis

Human IPSC nestin and β3 tubulin colocalization was performed using Sigma Plot 13.0. All other statistical analysis was carried out using Prism software. The data sets were first evaluated as parametric versus nonparametric using the Shapiro–Wilk normality test. The corresponding one-way analysis of variance (ANOVA) test was used when there were multiple comparisons, and the *t* test was used when only two conditions were compared. This is specified in the figure legends. Significance is denoted throughout with the following abbreviations: n.s. is not significant, $*p < 0.05$, $**p < 0.01$, $*** p < 0.001$, $****p < 0.0001$.

ACKNOWLEDGMENTS

We thank Brenna Kirk and Pranaya Pakala in the Litwa lab for work with human IPSCs, Meheret Kinfe and Lloyd McMahon in the Winckler lab for blinded neuron counting and morphology analysis, the Deppman lab at UVA for TUJ1 antibody, Laura Digilio, Lloyd McMahon, Kelly Barford (Winckler Lab), and Austin Keeler (Deppman lab) for help with manuscript revision and expertise, Zdenek Svindrych of the University of Virginia Keck Center for assistance with STED microscopy, and Bruce Lahn's laboratory at the University of Chicago for generously providing mouse nestin cDNA. This work was supported by National Institutes of Health (NIH) Grant R01NS081674 (to B.W.). C.B. was supported by an institutional NIH training grant (T32 GM008136).

REFERENCES

Argiro A, Bunge MB, Johnson IT, Rapp S, Scott B (1984). Correlation between growth form and movement and their dependence on neuronal age. J Neurosci 4, 3051–3062.

Arner E, Daub CO, Vitting-Seerup K, Andersson R, Lilje B, Drabløs F, Lennartsson A, Rönnerblad M, Hrydziuszko O, Vitezic M, *et al.* (2015). Transcribed enhancers lead waves of coordinated transcription in transitioning mammalian cells. Science 347, 1010–1015.

Astle MV, Ooms LM, Cole AR, Binge LC, Dyson JM, Layton MJ, Petratos S, Sutherland C, Mitchell CA (2011). Identification of a proline-rich inositol polyphosphate 5-phosphatase (PIPP)•collapsin response mediator protein 2 (CRMP2) complex that regulates neurite elongation. J Biol Chem 286, 23407–23418.

Banker GA, Cowan WM (1977). Rat hippocampal neurons in dispersed cell culture. Brain Res 126, 397–425.

Beher O, Golden JA, Mashimo H, Schoen F, Fishman M (1996). Semaphorin III is needed for normal patterning and growth of nerves, bones, and heart. Nature 383, 525–528.

Benson DL, Mandell JW, Shaw G, Banker G (1996). Compartmentation of alpha-internexin and neurofilament triplet proteins in cultured hippocampal neurons. J Neurocyt 25, 181–196.
Bigler RL, Kamande JW, Dumitru R, Niedringhaus M, Taylor AM (2017). Messenger RNAs localized to distal projections of human stem cell derived neurons. Sci Rep 7, 611–615.
Boyne LJ, Fischer I, Shea TB (1996). Role of vimentin in early stages of neuritogenesis in cultured hippocampal neurons. Int J Dev Neurosci 14, 739–748.
Brennand KJ, Simone A, Jou J, Gelboin-Burkhart C, Tran N, Sangar S, Li Y, Mu Y, Chen G, Yu D, *et al*. (2011). Modelling schizophrenia using human induced pluripotent stem cells. Nature 473, 221–225.
Brown M, Jacobs T, Eickholt B, Ferrari G, Teo M, Monfries C, Qi RZ, Leung T, Lim L, Hall C (2004). α2-Chimaerin, cyclin-dependent kinase 5/p35, and its target collapsin response mediator protein-2 are essential components in Semaphorin 3A-induced growth-cone collapse. J Neurosci 24, 8994–9004.
Carcea I, Ma'ayan A, Mesias R, Sepulveda B, Salton SR, Benson DL (2010). Flotillin-mediated endocytic events dictate cell type-specific responses to Semaphorin 3A. J Neurosci 30, 15317–15329.
Cattaneo E, McKay R (1990). Proliferation and differentiation of neuronal stem cells regulated by nerve growth factor. Nature 347, 762–765.
Chang L, Goldman RD (2004). Intermediate filaments mediate cytoskeletal crosstalk. Nat Rev Mol Cell Biol 5, 601–613.
Chen G, Sima J, Jin M, Wang KY, Xue XJ, Zheng W, Ding YQ, Yuan XB (2008). Semaphorin-3A guides radial migration of cortical neurons during development. Nat Neurosci 11, 36–44.
Chen HL, Yuh CH, Wu KK (2010). Nestin is essential for zebrafish brain and eye development through control of progenitor cell apoptosis. PLoS One 5, e9318–12.
Cochard P, Paulin D (1984). Initial expression of neurofilaments and vimentin in the central and peripheral nervous system of the mouse embryo in vivo. J Neurosci 4, 2080–2094.
Crews L, Patrick C, Adame A, Rockenstein E, Masliah E (2011). Modulation of aberrant CDK5 signaling rescues impaired neurogenesis in models of Alzheimer's disease. Cell Death Dis 2, e120-e123.
Crino PB, Eberwine J (1996). Molecular characterization of the dendritic growth cone: regulated mRNA transport and local protein synthesis. Neuron 17, 1173–1187.
Dahlstrand J, Lardelli M, Lendahl U (1995). Nestin mRNA expression correlates with the central nervous system progenitor cell state in many, but not all, regions of developing central nervous system. Dev Brain Res 84, 109–129.
Dang P, Smythe E, Furley AJW (2013). TAG1 regulates the endocytic trafficking and signalling of the Semaphorin3A receptor complex. J Neurosci 32, 10370–10382.
Decimo I, Bifari F, Rodriguez FJ, Malpeli G, Dolci S, Lavarini V, Pretto S, Vasquez S, Sciancalepore M, Montalbano A, *et al*. (2011). Nestin- and doublecortin-positive cells reside in adult spinal cord meninges and participate in injury-induced parenchymal reaction. Stem Cells 29, 2062–2076.
Dent EW, Barnes AM, Tang F, Kalil K. (2004). Netrin-1 and Semaphorin 3A promote or inhibit cortical axon branching, respectively, by reorganization of the cytoskeleton. J Neurosci 24, 3002–3012.
Dey A, Farzanehfar P, Gazina EV, Aumann TD (2017). Electrophysiological and gene expression characterization of the ontogeny of nestin-expressing cells in the adult mouse midbrain. Stem Cell Res 23, 143–153.
Di CG, Xiang AP, Jia L, Liu JF, Lahn BT, Ma BF (2014). Involvement of extracellular factors in maintaining self-renewal of neural stem cell by nestin. Neuroreport 25, 782–787.
Digilio L, Yap CC, Winckler B (2015). Ctip2-, Satb2-, Prox1-, and GAD65-expressing neurons in rat cultures: preponderance of single- and double-positive cells, and cell type-specific expression of neuron-specific gene family members, Nsg-1 (NEEP21) and Nsg-2 (P19). PLoS One 10, e0140010.
Dotti CG, Sullivan CA, Banker GA (1988). The establishment of polarity by hippocampal neurons in culture. J Neurosci 8, 1454–1468.
Farzanehfar P, Horne MK, Aumann TD (2017a). An investigation of gene expression in single cells derived from nestin-expressing cells in the adult mouse midbrain in vivo. Neurosci Lett 648, 34–40.
Farzanehfar P, Lu SS, Dey A, Musiienko D, Baagil H, Horne MK, Aumann TD (2017b). Evidence of functional duplicity of nestin expression in the adult mouse midbrain. Stem Cell Res 19, 82–93.
Fliegner KH, Kaplan MP, Wood TL, Pintar JE, Liem RK (1994). Expression of the gene for the neuronal intermediate filament protein alpha-internexin coincides with the onset of neuronal differentiation in the developing rat nervous system. J Comp Neurol 342, 161–173.
Francis F, Koulakoff A, Boucher D, Chafey P, Schaar B, Vinet MC, Friocourt G, McDonnell N, Reiner O, Kahn A, *et al*. (1999). Doublecortin is a developmentally regulated, microtubule-associated protein expressed in migrating and differentiating neurons. Neuron 23, 247–256.
Grabham PW, Seale GE, Bennecib M, Goldberg DJ, Vallee RB (2007). Cytoplasmic dynein and LIS1 are required for microtubule advance during growth cone remodeling and fast axonal outgrowth. J Neurosci 27, 5823–5834.
Gu H, Wang S, Messam CA, Yao Z (2002). Distribution of nestin immunoreactivity in the normal adult human forebrain. Brain Res 943, 174–180.
Guo KH, Li DP, Gu HY, Jie-Xu, Yao ZB (2014). Postnatal development of nestin positive neurons in rat basal forebrain: different onset and topography with choline acetyltransferase and parvalbumin expression. Int J Dev Neurosci 35, 72–79.
Hemmati-Brivanlou A, Mann RW, Harland RM (1992). A protein expressed in the growth cones of embryonic nerves defines a new class of intermediate filament protein. Neuron 9, 417–428.
Hendrickson ML, Rao AJ, Demerdash ON, Kalil RE (2011). Expression of nestin by neural cells in the adult rat and human brain. PLoS One 6, e18535.
Henley JR, Huang KH, Wang D, Poo MM (2004). Calcium mediates bidirectional growth cone turning induced by myelin-associated glycoprotein. Neuron 44, 909–916.
Hockfield S, McKay RD (1985). Identification of major cell classes in the developing mammalian nervous system. J Neurosci 5, 3310–3328.
Hu W, Lu H, Wang S, Yin W, Liu X, Dong L, Chiu R, Shen L, Lu WJ, Lan F (2016). Suppression of nestin reveals a critical role for p38-EGFR pathway in neural progenitor cell proliferation. Oncotarget 7, 87052–87063.
Hughes AJ, Spelke DP, Xu Z, Kang CC, Schaffer DV, Herr AE (2014). Single-cell Western blotting. Nat Methods 11, 455–464.
Hyder CL, Lazaro G, Pylvänäinen JW, Roberts MW, Qvarnström SM, Eriksson JE (2014). Nestin regulates prostate cancer cell invasion by influencing the localisation and functions of FAK and integrins. J Cell Sci 127, 2161–2173.
Ip JP, Shi L, Chen Y, Itoh Y, Fu WY, Betz A, Yung WH, Gotoh Y, Fu AK, Ip NY (2011). α 2-Chimaerin controls neuronal migration and functioning of the cerebral cortex through CRMP-2. Nat Neurosci 15, 39–47.
Kaplan A, Kent CB, Charron F, Fournier AE (2014). Switching responses: spatial and temporal regulators of axon guidance. Mol Neurobiol 49, 1077–1086.
Kaplan MP, Chin SS, Fliegner KH, Liem RK (1990). α-Internexin, a novel neuronal intermediate filament protein, precedes the low molecular weight neurofilament protein (NF-L) in the developing rat brain. J Neurosci 10, 2735–2748.
Kawauchi T (2014). Cdk5 regulates multiple cellular events in neural development, function and disease. Dev Growth Differ 56, 335–348.
Kent CB, Shimada T, Ferraro GB, Ritter B, Yam PT, McPherson PS, Charron F, Kennedy TE, Fournier AE (2010). 14-3-3 proteins regulate protein kinase A activity to modulate growth cone turning responses. J Neurosci 30, 14059–14067.
Khazaei MR, Girouard MP, Alchini R, Ong Tone S, Shimada T, Bechstedt S, Cowan M, Guillet D, Wiseman PW, Brouhard G, *et al*. (2014). Collapsin response mediator protein 4 regulates growth cone dynamics through the actin and microtubule. J Biol Chem 289, 30133–30143.
Kolodkin AL, Tessier-Lavigne M (2011). Mechanisms and molecules of neuronal wiring: a primer. Cold Spring Harb Perspect Biol 3, a001727.
Kuo LT, Simpson A, Schänzer A, Tse J, An SF, Scaravilli F, Groves MJ (2005). Effects of systemically administered NT-3 on sensory neuron loss and nestin expression following axotomy. J Comp Neurol 482, 320–332.
Lariviere RC, Julien J (2003). Functions of intermediate filaments in neuronal development and disease. J Neurobiol 58, 131–148.
Leduc C, Manneville SE (2017). Regulation of microtubule-associated motors drives intermediate filament network polarization. J Cell Biol 216, 1689–1703.
Lee S, Shea TB (2014). The high molecular weight neurofilament subunit plays an essential role in axonal outgrowth and stabilization. Biol Open 3, 974–981.
Lendahl U, Zimmerman LB, McKay RDG (1990). CNS stem cells express a new class of intermediate filament protein. Cell 60, 585–595.
Liang ZW, Wang Z, Chen H, Li C, Zhou T, Yang Z, Yang X, Yang Y, Gao G, Cai W (2015). Nestin-mediated cytoskeletal remodeling in endothelial cells: novel mechanistic insight into VEGF-induced cell migration in angiogenesis. Am J Physiol Cell Physiol 308, C349–C358.

Lin W, Dominguez B, Yang J, Aryal P, Brandon EP, Gage FH, Lee KF (2005). Neurotransmitter acetylcholine negatively regulates neuromuscular synapse formation by a Cdk5-dependent mechanism. Neuron 46, 569–579.
Liu J, Reeves C, Jacques T, McEvoy A, Miserocchi A, Thompson P, Sisodiya S, Thom M (2018). Nestin-expressing cell types in the temporal lobe and hippocampus: morphology, differentiation, and proliferative capacity. Glia 66, 62–77.
Messam CA, Hou J, Berman JW, Major EO (2002). Analysis of the temporal expression of nestin in human fetal brain derived neuronal and glial progenitor cells. Dev Brain Res 134, 87–92.
Messam CA, Hou J, Major EO (1999). Coexpression of nestin in neural and glial cells in the developing human CNS defined by a human-specific anti-nestin antibody. Exp Neurol 161, 585–596.
Miller FD, Gauthier AS (2007). Timing is everything: making neurons versus glia in the developing cortex. Neuron 54, 357–369.
Mintz CD, Carcea I, McNickle DG, Dickson TC, Ge Y, Salton SR, Benson DL (2008). ERM proteins regulate growth cone responses to Sema3A. J Comp Neurol 510, 351–366.
Mohseni P, Sung HK, Murphy AJ, Laliberte CL, Pallari HM, Henkelman M, Georgiou J, Xie G, Quaggin SE, Thorner PS, *et al.* (2011). Nestin is not essential for development of the CNS but required for dispersion of acetylcholine receptor clusters at the area of neuromuscular junctions. J Neurosci 31, 11547–11552.
Namba T, Kibe Y, Funahashi Y, Nakamuta S, Takano T, Ueno T, Shimada A, Kozawa S, Okamoto M, Shimoda Y, *et al.* (2014). Pioneering axons regulate neuronal polarization in the developing cerebral cortex. Neuron 81, 814–829.
Narita K, Matsuda Y, Seike M, Naito Z, Gemma A, Ishiwata T (2014). Nestin regulates proliferation, migration, invasion and stemness of lung adenocarcinoma. Int J Oncol 44, 1118–1130.
Ng T, Ryu JR, Sohn JH, Tan T, Song H, Ming GL, Goh EL (2013). Class 3 Semaphorin mediates dendrite growth in adult newborn neurons through Cdk5/FAK pathway. PLoS One 8, 1–15.
Pacey L, Stead S, Gleave JA, Tomczyk K, Doering LC (2006). Neural stem cell culture: neurosphere generation, microscopical analysis and cryopreservation. Nature Protocol Exchange doi:10.1038/nprot.2006.215.
Pallari HM, Lindqvist J, Torvaldson E, Ferraris SE, He T, Sahlgren C, Eriksson JE (2011). Nestin as a regulator of Cdk5 in differentiating myoblasts. Mol Biol Cell 22, 539–1551.
Park D, Xiang AP, Mao FF, Zhang L, Di CG, Liu XM, Shao Y, Ma BF, Lee JH, Ha KS, *et al.* (2010). Nestin is required for the proper self-renewal of neural stem cells. Stem Cells 28, 2162–2171.
Perlini LE, Szczurkowska J, Ballif BA, Piccini A, Sacchetti S, Giovedì S, Benfenati F, Cancedda L (2015). Synapsin III acts downstream of Semaphorin 3A/CDK5 signaling to regulate radial migration and orientation of pyramidal neurons in vivo. Cell Rep 11, 234–248.
Perry EK, Johnson M, Ekonomou A, Perry RH, Ballard C, Attems J (2012). Neurogenic abnormalities in Alzheimer's disease differ between stages of neurogenesis and are partly related to cholinergic pathology. Neurobiol Dis 47, 155–162.
Polleux F, Morrow T, Ghosh A (2000). Semaphorin 3A is a chemoattractant for cortical apical dendrites. Nature 404, 567–573.
Poulain FE, Sobel A (2007). The "SCG10-like protein" SCLIP is a novel regulator of axonal branching in hippocampal neurons, unlike SCG10. Mol Cell Neurosci 34, 137–146.
Ren Y, Suter DM (2016). Increase in growth cone size correlates with decrease in neurite growth rate. Neural Plast doi.org/10.1155/2016/3497901.
Romito-DiGiacomo RR, Menegay H, Cicero SA, Herrup K (2007). Effects of Alzheimer's disease on different cortical layers: the role of intrinsic differences in Abeta susceptibility. J Neurosci 27, 8496–504.
Ruediger T, Zimmer G, Barchmann S, Castellani V, Bagnard D, Bolz J (2013). Integration of opposing Semaphorin guidance cues in cortical axons. Cereb Cortex 23, 604–614.
Sahlgren CM, Mikhailov A, Vaittinen S, Pallari HM, Kalimo H, Pant HC, Eriksson JE (2003). Cdk5 regulates the organization of nestin and its association with p35. Mol Cell Biol 23, 5090–5106.
Sahlgren CM, Pallari HM, He T, Chou YH, Goldman RD, Eriksson JE (2006). A nestin scaffold links Cdk5/p35 signaling to oxidant-induced cell death. EMBO J 25, 4808–1819.
Sasaki Y, Cheng C, Uchida Y, Nakajima O, Ohshima T, Yagi T, Taniguchi M, Nakayama T, Kishida R, Kudo Y (2002). Fyn and Cdk5 mediate Semaphorin-3A signaling, which is involved in regulation of dendrite orientation in cerebral cortex. Neuron 35, 907–920.
Shea TB, Beermann ML (1999). Neuronal intermediate filament protein alpha-internexin facilitates axonal neurite elongation in neuroblastoma cells. Cell Motil Cytoskeleton 43, 322–333.
Shea TB, Beermann ML, Fischer I (1993). Transient requirement for vimentin in neuritogenesis: intracellular delivery of anti-vimentin antibodies and antisense oligonucleotides inhibit neurite initiation but not elongation of existing neurites in neuroblastoma. J Neurosci Res 76, 66–76.
Shelly M, Cancedda L, Lim BK, Popescu AT, Cheng PL, Gao H, Poo MM (2011). Semaphorin3A regulates neuronal polarization by suppressing axon formation and promoting dendrite growth. Neuron 71, 433–445.
Shinmyo Y, Riyadh MA, Ahmed G, Naser NB, Hossain M, Takebayashi H, Kawasaki H, Ohta K, Tanaka H (2015). Draxin from neocortical neurons controls the guidance of thalamocortical projections into the neocortex. Nature Comm 6, 10232.
Sibbe M, Taniguchi M, Schachner M, Bartsch U (2007). Development of the corticospinal tract in Semaphorin3A- and cd24-deficient mice. Neurosci 150, 898–904.
Steinert PM, Chou YH, Prahlad V, Parry DA, Marekov LN, Wu KC, Jang SI, Goldman RD (1999). A high molecular weight intermediate filament-associated protein in BHK-21 cells is nestin, a type VI intermediate filament protein: limited co-assembly in vitro to form heteropolymers with type III vimentin and type IV alpha-internexin. J Biol Chem 274, 9881–9890.
Su PH, Chen CC, Chang YF, Wong ZR, Chang KW, Huang BM, Yang HY (2013). Identification and cytoprotective function of a novel nestin isoform, Nes-S, in dorsal root ganglia neurons. J Biol Chem 288, 8391–404.
Takano T, Xu C, Funahashi Y, Namba T, Kaibuchi K (2015). Neuronal polarization. Development 142, 2088–2093.
Telley L, Govindan S, Prados J, Stevant I, Nef S, Dermitzakis E, Dayer A, Jabaudon D (2016). Sequential transcriptional waves direct the differentiation of newborn neurons in the mouse neocortex. Science 351, 1443–1446.
Tojima T, Itofusa R, Kamiguchi H (2014). Steering neuronal growth cones by shifting the imbalance between exocytosis and endocytosis. J Neurosci 34, 7165–7178.
Toth C, Shim SY, Wang J, Jiang Y, Neumayer G, Belzil C, Liu WQ, Martinez J, Zochodne D, Nguyen MD (2008). Ndel1 promotes axon regeneration via intermediate filaments. PLoS One 3, e214-e222.
Vitriol EA, Zheng JQ (2012). Growth cone travel in space and time: the cellular ensemble of cytoskeleton, adhesion, and membrane. Neuron 73, 1068–1080.
Walker KL, Yoo HK, Undamatla J, Szaro BG (2001). Loss of neurofilaments alters axonal growth dynamics. J Neurosci 21, 9655–9666.
Walker TL, Yasuda T, Adams DJ, Bartlett PF (2007). The doublecortin-expressing population in the developing and adult brain contains multipotential precursors in addition to neuronal-lineage cells. J Neurosci 27, 3734–3742.
Wang L, Ho CL, Sun D, Liem RK, Brown A (2000). Rapid movement of axonal neurofilaments interrupted by prolonged pauses. Nat Cell Biol 2, 137–141.
Wang X, Sterne GR, YE B (2014). Regulatory mechanisms underlying the differential growth of dendrites and axons. Neurosci Bull 30, 557–568.
Wei LC, Shi M, Cao R, Chen LW, Chan YS (2008). Nestin small interfering RNA (siRNA) reduces cell growth in cultured astrocytoma cells. Brain Res 1196, 103–112.
Wilhelmsson U, Lebkuechner I, Leke R, Marasek P, Yang X, Antfolk D, Chen M, Mohseni P, Lasic E, Bobnar ST, *et al.* (2019). Nestin regulates neurogenesis in mice through notch signaling from astrocytes to neural stem cells. Cereb Cortex 12, 269–17.
Xue X, Yuan X (2010). Nestin is essential for mitogen-stimulated proliferation of neural progenitor cells. Mol Cell Neurosci 45, 26–36.
Yabe JT, Chan WK, Wang FS, Pimenta A, Ortiz DD, Shea TB (2003). Regulation of the transition from vimentin to neurofilaments during neuronal differentiation. Cell Motil Cytoskeleton 56, 193–205.
Yam PT, Kent CB, Morin S, Farmer WT, Alchini R, Lepelletier L, Colman DR, Tessier-Lavigne M, Fournier AE, Charron F (2012). 14-3-3 proteins regulate a cell-intrinsic switch from sonic hedgehog-mediated commissural axon attraction to repulsion after midline crossing. Neuron 76,735–749.
Yan S, Li P, Wang Y, Yu W, Qin A, Liu M, Xiang AP, Zhang W, Li W (2016). Nestin regulates neural stem cell migration via controlling the cell contractility. Int J Biochem Cell Biol 78, 349–360.

Yan Y, Yang J, Bian W, Jing N (2001). Mouse nestin protein localizes in growth cones of P19 neurons and cerebellar granule cells. Neurosci Lett 302, 89–92.
Yang J, Dominguez B, de Winter F, Gould TW, Eriksson JE, Lee KF (2011). Nestin negatively regulates postsynaptic differentiation of the neuromuscular synapse. Nat Neurosci 14, 324–330.
Zhang J, Zhong J, Yu J, Li J, Di W, Lu P, Yang X, Zhao W, Wang X, Su W (2017). Nestin expression involves invasiveness of esophageal carcinoma and its downregulation enhances paclitaxel sensitivity to esophageal carcinoma cell apoptosis. Oncotarget 8, 65056–65063.
Zhao Z, Lu P, Zhang H, Xu H, Gao N, Li M, Liu C (2014). Nestin positively regulates the Wnt/β-catenin pathway and the proliferation, survival and invasiveness of breast cancer stem cells. Breast Cancer Res 16, 408–413.
Zhou J, Wen Y, She L, Sui YN, Liu L, Richards LJ, Poo MM (2013). Axon position within the corpus callosum determines contralateral cortical projection. Proc Natl Acad Sci USA 110, E2714–E2723.
Zhu J, Gu H, Yao Z, Zou J, Guo K, Li D, Gao T (2011). The nestin-expressing and non-expressing neurons in rat basal forebrain display different electrophysiological properties and project to hippocampus. BMC Neurosci 12, 129–133.

Supplemental Materials

Molecular Biology of the Cell

Bott et al.

Supplementary Figure 1

A. Nestin knockdown was also qualitatively assessed by western blotting of whole cell lysates of cortical cultures (1 DIV) with Mouse, Goat, and Chicken nestin antibodies. A band of the expected size was detected with all 3 antibodies in siCon but decreased levels are seen after siNes expression. The knockdown was partial. This is likely due to lower transfection efficiencies in cultured neurons where less than 50% of cells are transfected. The related intermediate filament vimentin was unaffected, and DCX was blotted as a loading control.

A'. Myc-tagged nestin was overexpressed in HEK293 cells and co-transfected using lipofectamine2000 with siCon or siNes siRNA. Lysates were blotted for the myc-tag and for nestin, demonstrating near complete knockdown in the high transfection efficiency HEK293 cells. The related intermediate filament vimentin was unaffected, and alpha-tubulin is loading control.

B and B'. Full blots demonstrating specificity of nestin antibodies used in IF studies as a single band above 250 kd (~300kd). Protein lysate from cultured 1DIV E16 mouse neurons (B), and E16 mouse cortex (B'), both probed with the goat anti-Nestin antibody and the mouse anti-Nestin clone 2q178 antibody. In addition, E16 brain lysates were probed in the presence or absence of the immunizing peptide to the goat nestin antibody. This preincubation specifically diminished the ~300kd immunoreactive band recognized by the goat antibody.

C. Side by side comparison of nestin levels in a Sox2 positive neural progenitor cell (NPC) and a primary differentiating DCX positive neuron. E16 mouse cortical cultures at 1DIV were stained with antibodies to the indicated proteins. They contain mostly neurons but an occasional NPC can still be found at 1 DIV. Nestin levels in the in the primary neurite and cell body of DCX+ neurons are many fold lower than in the NPC, but is still detectable.

Supplementary Figure 2

A. Nestin is expressed in βIII tubulin-positive neurons in human IPSC derived mini-brains. The boxed regions 1-3 are shown larger in the insets, and arrowheads indicate nestin βIII tubulin doublepositive cells. Nestin positive radial glia like cells span the spheroid, while high βIII tubulin cells are located to the periphery. Low βIII tubulin expressing cells can also be found in the central ventricular-like region representing differentiating neurons not yet migrated, and insets analyzed are outside of this region. Nestin can be detected in the tips of some of the βIII tubulin processes (arrowheads).

B. Both nestin negative and nestin positive have a range of Ctip2 and Satb2 nuclear intensities. Pink arrowheads indicate nestin in the distal axon. A total of 68 DCX+ neurons (24 nestin negative, 44 nestin positive) were quantified in terms of nuclear

intensity of either Ctip2 or Stab2 immunostaining. No correlation was found. (Unpaired t-test)

Supplementary Figure 3

A,B. Nestin (multiple antibodies) is found together with its polymerization partner vimentin along axons (identified by the axonal cell adhesion molecule L1-CAM). Arrow heads indicate radial glia and arrows indicate nestin-positive axons.
Both the mouse anti-nestin antibody 2q178 (A) and rat401 (B) produce similar axon immunostaining in E16 mouse cortex, as do the other nestin antibodies used in this study (Figure 3b).

Supplementary Figure 4

A. Relative efficiency of nestin silencing of the 4 individual siRNA's from the siNes pool. Myc-tagged nestin was overexpressed in HEK 293 cells and co-transfected using lipofectamine 2000 with siCon or various siNes siRNA. Lane 1 is untransfected HEK293 cell lysate. Lysates were blotted for the myc-tag and for nestin, demonstrating again complete knockdown with the siNes pool, as well as efficient knockdown by siNes #1 and 17. siNes #3 had an intermediate effect, while siNes #4 was the least effective, and is used as an additional control in the following experiments in neurons. The related intermediate filament vimentin was unaffected, and α-tubulin is used as a loading control.

B-E. 3 individual siNes siRNA's were transfected into neurons to confirm efficiency (B) and confirm morphological phenotypes (C,D,E) seen after nestin depletion by siNes pool. Both effective siNes #1 and #17 (and the siNes-pool) resulted in a significant depletion of nestin positive neurons after 36 hours, while the non-effective siNes #4 did not significantly reduce the number of nestin positive cells. None of the transfection conditions altered the average axon length (C), while siNes #1 and #17 phenocopied the pool by growth cone area (D) and growth cone filopodia number (E), while siNes #4 had no significant effect. Error bars are SEM. N=3 experiments, with the means of each plotted on the graph. Normality was confirmed with the shapiro-Wilk normality test. Each condition was compared to control with a one way ANOVA with Dunnet's correction.

F. A labeled version of the cell in Figure 5E diagraming how morphological measurements were made.

Supplementary Figure 1

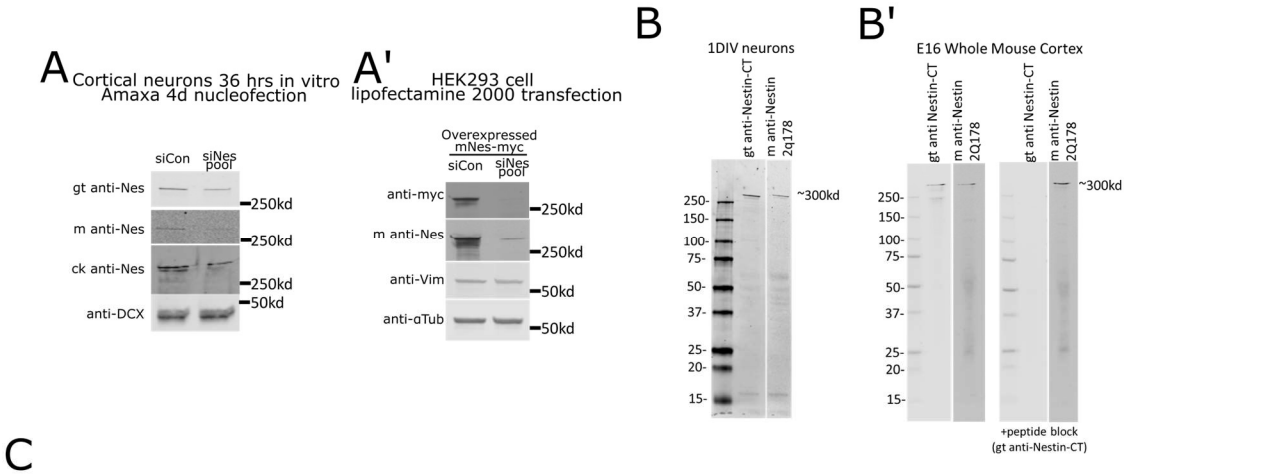

C

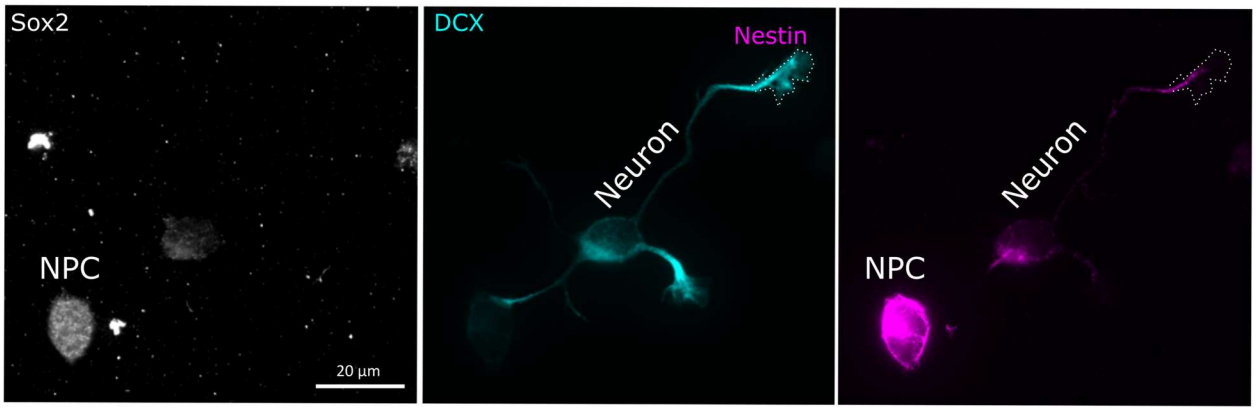

Supplementary Figure 2

A Nestin in Human IPSC derived minibrains

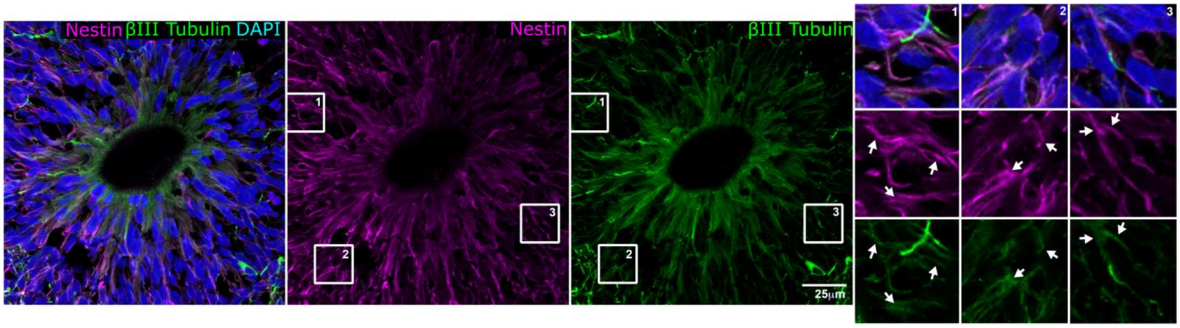

B

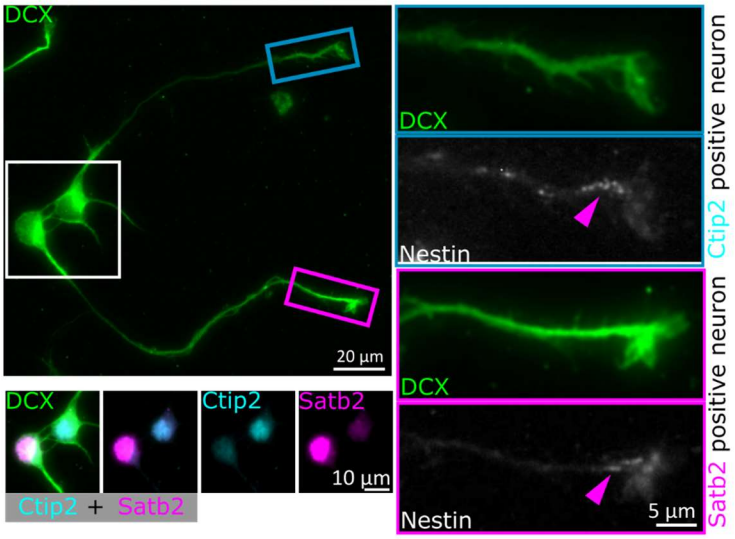

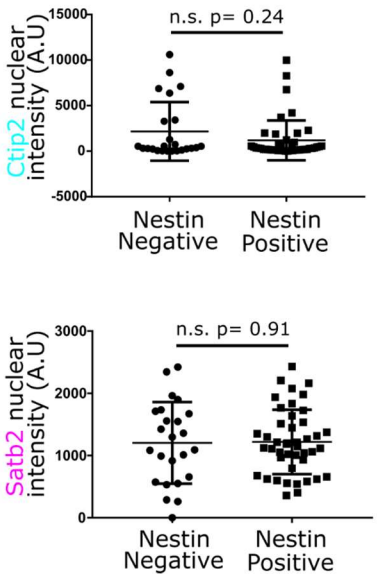

Supplementary Figure 3

A

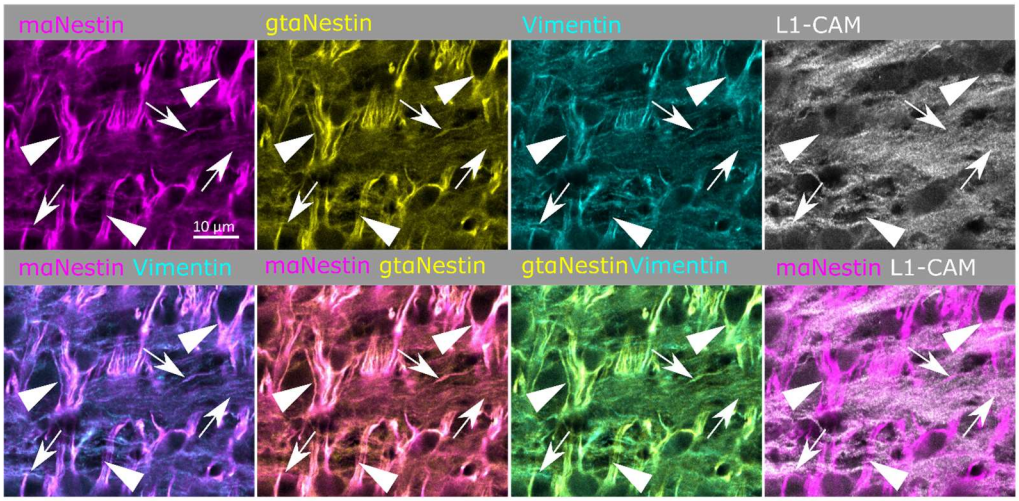

B

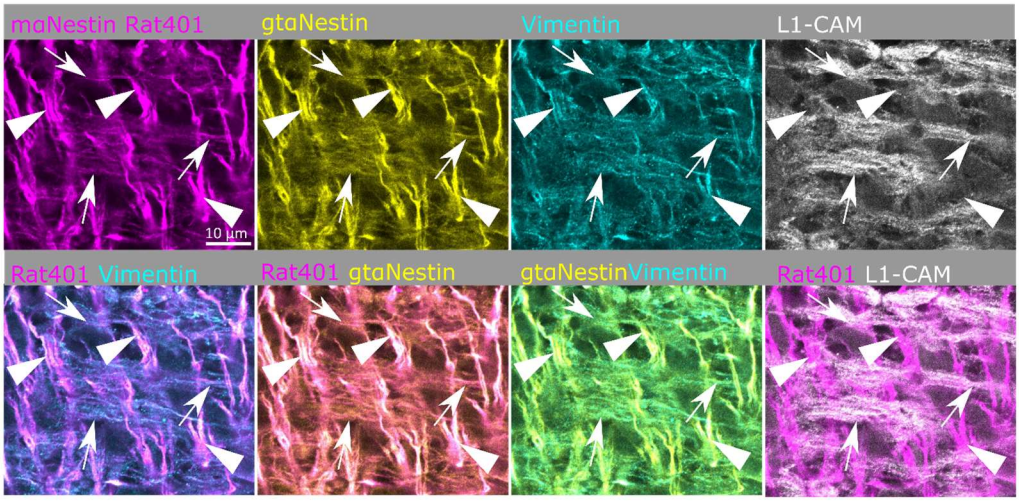

Supplementary Figure 4

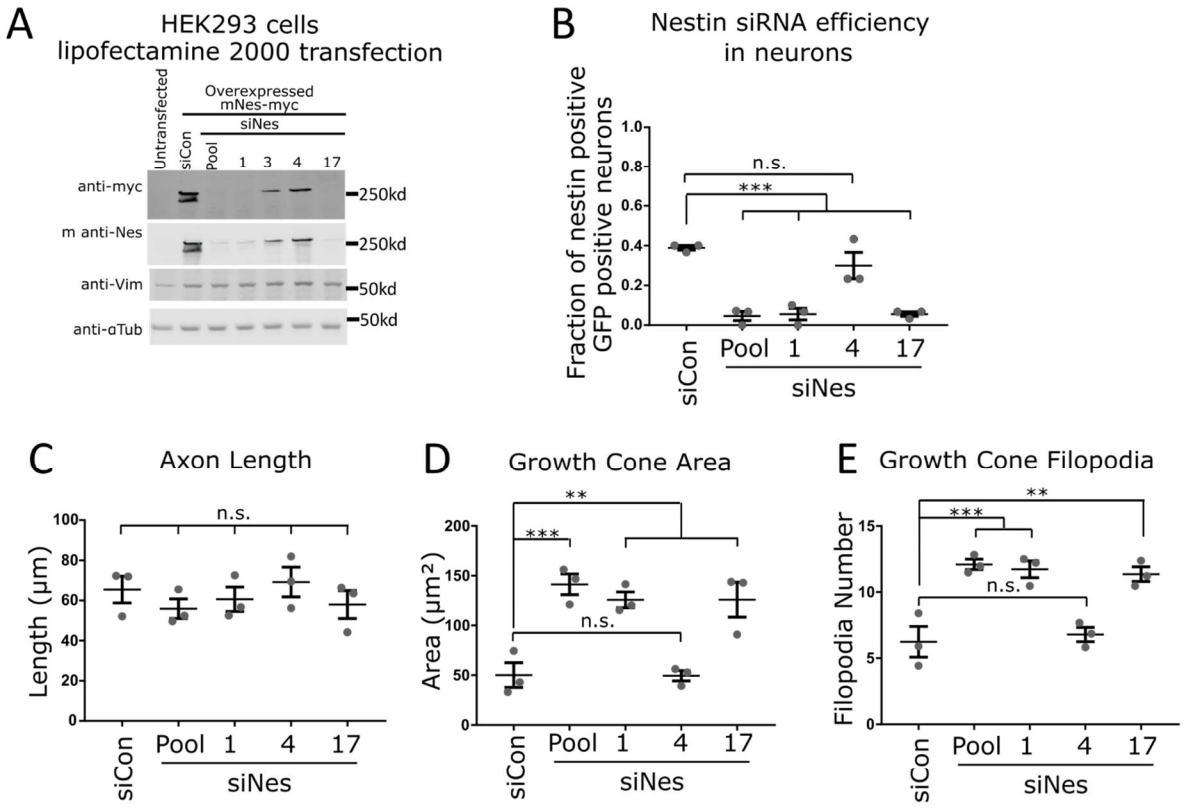

F Diagram of morphology measurements